Hindawi
Journal of Chemistry
Volume 2023, Article ID 5413236, 20 pages
https://doi.org/10.1155/2023/5413236

Research Article

Novel Thiosemicarbazone Derivatives from Furan-2-Carbaldehyde: Synthesis, Characterization, Crystal Structures, and Antibacterial, Antifungal, Antioxidant, and Antitumor Activities

Wilfredo Hernández,[1] **Fernando Carrasco**,[1] **Abraham Vaisberg**,[2] **Evgenia Spodine**,[3] **Maik Icker**,[4] **Harald Krautscheid**,[4] **Lothar Beyer**,[4] **Carmen Tamariz-Angeles**,[5] **and Percy Olivera-Gonzales**[5]

[1]*Facultad de Ingeniería, Universidad de Lima, Av. Javier Prado Este 4600, Lima 33, Peru*
[2]*Laboratorios de Investigación y Desarrollo, Facultad de Ciencias e Ingeniería, Universidad Peruana Cayetano Heredia, Av. Honorio Delgado 430, Lima 31, Peru*
[3]*Facultad de Ciencias Químicas y Farmacéuticas, Universidad de Chile, Olivos 1007, Casilla 233, Independencia, Santiago 8330492, Chile*
[4]*Fakultät für Chemie und Mineralogie, Universität Leipzig, Johannisallee 29 D-04103, Leipzig, Germany*
[5]*Centro de Investigación de la Biodiversidad y Recursos Genéticos de Ancash, Facultad de Ciencias, Universidad Nacional Santiago Antúnez de Mayolo, Av. Centenario 200, Independencia, Huaraz 02002, Ancash, Peru*

Correspondence should be addressed to Wilfredo Hernández; whernandez79@yahoo.es, Evgenia Spodine; espodine@ciq.uchile.cl, and Maik Icker; maik.icker@uni-leipzig.de

Received 12 March 2023; Revised 18 July 2023; Accepted 3 August 2023; Published 14 September 2023

Academic Editor: Narcis Avarvari

Ten new thiosemicarbazone derivatives, furan-2-carbaldehyde thiosemicarbazone (**1**), 3-methyl-furan-2-carbaldehyde thiosemicarbazone (**2**), 5-hydroxymethyl-furan-2-carbaldehyde thiosemicarbazone (**3**), 5-trifluoromethyl-furan-2-carbaldehyde thiosemicarbazone (**4**), 5-nitro-furan-2-carbaldehyde thiosemicarbazone (**5**), 5-phenyl-furan-2-carbaldehyde thiosemicarbazone (**6**), 5-(2-fluorophenyl)-furan-2-carbaldehyde thiosemicarbazone (**7**), 5-(4-methoxyphenyl)-furan-2-carbaldehyde thiosemicarbazone (**8**), 5-(1-naphthyl)-furan-2-carbaldehyde thiosemicarbazone (**9**), and 5-(1H-Pyrazol-5-yl)-furan-2-carbaldehyde thiosemicarbazone (**10**) were synthesized by condensing thiosemicarbazide with the respective furan-2-carbaldehyde in methanol. The prepared compounds were characterized by spectroscopic studies (FT-IR and NMR) and electrospray mass spectrometry. The molecular structures of **2**, **6**, **7,** and **8** have also been determined by X-ray crystallography. Compounds **2**, **6,** and **7** crystallize in the *E* conformation about the N1-C6, N1-C11, and N1-C11 bonds, respectively, while 8 adopts the *Z* conformation about the N1-C12 bond with the presence of an intramolecular N2-H. . .O2 hydrogen bond. All prepared thiosemicarbazone derivatives were evaluated for their in vitro antibacterial, antifungal, and antitumor activities against *Staphylococcus aureus* strains, *Candida albicans*/*Candida tropicalis* fungi, and seven human tumor cell lines (HuTu80, H460, DU145, M-14, HT-29, MCF-7, and LNCaP), respectively. The antioxidant activity was also studied by the DPPH assay. Compound **5** exhibited significant antibacterial activity against *Staphylococcus aureus* ATCC700699 (MIC = 1 μg/mL) compared to the nitrofurantoin and gentamicin reference drugs (MIC = 1–25 and 10->100 μg/mL, respectively). Compound **4** was ten times less active than amphotericin B (MIC = 5 μg/mL) against *Candida albicans* (ATCC90028 and ATCC10231), while **1** exhibited a moderate effect of scavenging of DPPH radical (IC_{50} = 40.9 μg/mL) in comparison to ascorbic acid reference compound (IC_{50} = 22.0 μg/mL). Among all the studied thiosemicarbazones, **5** showed a higher cytotoxic activity (IC_{50} = 13.36–27.73 μM) in relation to the other tested compounds (IC_{50} = 34.84—>372.34 μM) against all tested cell lines, except the LNCaP cell line, exhibiting its highest antiproliferative activity (IC_{50} = 13.36 μM) on the HuTu80 cell line. Besides, **8** and **9** exhibited high antitumor activity (IC_{50} = 13.31 and 7.69 μM, respectively) against the LNCaP cells.

1. Introduction

The interest in preparing new thiosemicarbazone derivatives of general formula R-CH=N-NHCSNHR[1] has attracted the attention of researchers in the area of organic and coordination chemistry, due to the ease of carrying out the reaction between different aldehyde groups (R-CHO) or ketones (R–CO–R′) with derivatives from thiosemicarbazide ($NH_2NHCSNHR^1$) to obtain a broad spectrum of new thiosemicarbazone derivatives. These compounds which contain N and S atoms usually act as bidentate or multidentate chelating ligands and can coordinate to transition metal ions through the sulfur and hydrazine nitrogen atoms [1]. Extensive investigations conducted by researchers have demonstrated that metal complexes with some thiosemicarbazone derivatives present a wide range of biological applications, such as antibacterial [2, 3], antifungal [1, 4], antiparasitic [5], antitubercular [6, 7], antiviral [8, 9], antioxidant [10, 11], and antitumoral activities [12–14].

Numerous investigations have been carried out with α(N)-heterocyclic thiosemicarbazones because some of them act as potential antitumor agents. The biochemical mechanism of action is due to the ability of these compounds in inhibiting the enzyme ribonucleoside diphosphate reductase (RDR) which is responsible for the synthesis of DNA precursors [15, 16]. Evidence of this finding has been reported for Triapine (3-aminopyridine-2-carboxaldehyde thiosemicarbzone), a compound that inhibits the tumor cell growth at nanomolar concentrations and is being investigated in clinical trials (Phase 1 and Phase 2) for the treatment of cervical cancer [12]. Besides, Triapine has chelating properties and forms coordination compounds with iron ions [17]. Probably, the formation of redox-active iron complexes is a crucial step of the mechanism of action [18].

It has been demonstrated that compounds (+)-(*R*)-*N*(1)-(furan-2-yl-methylene)]-*N*(4)-[2-(4-methylcyclohex-3-en-1-yl)-propan-2-yl]- thiosemicarbazide ($GI_{50} = 3.3\,\mu$g/mL) and (−)-(*S*)-*N*(1)-(furan-2-yl-methylene)]-*N*(4)-[2-(4-methylcyclohex-3-en-1-yl)-propan-2-yl]-thiosemicarbazide ($GI_{50} = 5.8\,\mu$g/mL) show moderate activity against the lung (NCI-H460) and breast (MCF-7) human tumor cell lines compared to the doxorubicin antineoplastic drug of clinical use ($GI_{50} = 1.1–1.2\,\mu$g/mL) [19]. This evidence demonstrated that the presence of the *R*-(+)- and *S*-(−)-limonene fragments on the terminal amine of the thiosemicarbazone derivative increased their cytotoxic effect. On the other hand, it has been reported that 2-(1-(4-methyl- 2-(2-(1-(thiophen-2-yl) ethylidene) hydrazinyl) thiazol- 5-yl) ethylidene) hydrazinecarbothio-amide ($IC_{50} = 76.4\,\mu$M) exhibits an acceptable activity against MCF-7 cells in relation to cisplatin ($IC_{50} = 13.6\,\mu$M) [20]. On the other hand, 2-acetylthiophene thiosemicarbazone ($IC_{50} = 8.6\,\mu$M) was more active than cisplatin (($IC_{50} = 11.9\,\mu$M) against the HT-29 human colon adenocarcinoma cell line [21].

We have earlier reported the *in vitro* antiproliferative activity of pyridine-2-carbaldehyde thiosemicarbazone derivatives, assayed against certain types of human tumor cell lines. The obtained results indicated that the organic derivative 6-(1-trifluoroethoxy) pyridine-3-carbaldehyde thiosemicarbazone showed antiproliferative activity ($IC_{50} = 3.36\,\mu$M) greater than the 5-fluorouracile antineoplastic drug ($IC_{50} = 7.51\,\mu$M) against the M-14 amelanotic melanoma cell line [22]. This evidence revealed that the compound´s antiproliferative effect increased when the substituent group OCH_2CF_3 is at the 6-position of the pyridine ring. On the other hand, it has been reported that N(4)-methyl-2-acetylthiophene thiosemicarbazone ($MIC = 39.68\,\mu$g/mL) shows acceptable activity against *Staphylococcus aureus* ATCC 6538, as compared to the reference drug Ciprofloxacin ($MIC = 0.62\,\mu$g/mL) [23]. However, 2-acetylpyrazine N(4)-phenylthiosemicarbazone ($MIC = 500\,\mu$g/mL) and 2,5-dimethyl-3-acetylpyrazine thiosemicarbazone ($MIC = 512\,\mu$g/mL) were inactive against *S. aureus* with respect to ciprofloxacin ($MIC = 0.5\,\mu$g/mL) and chloramphenicol ($MIC = 32\,\mu$g/mL) antibacterial drugs [24, 25]. Besides, it was shown that compound 2-((5-nitrothiophen-2-yl) methylene)-N-(pyridin-3-yl) hydrazine carbothioamide ($MIC = 2.0–128.0\,\mu$g/mL) inhibited the growth of *C. albicans* strains [26].

Due to the broad spectrum of biological applications of thiosemicarbazones containing heterocyclic groups, our research group presents the preparation and characterization of new compounds derived from R-furan-2-carbaldehyde thiosemicarbazone (R = H, CH_3, CH_2OH, CF_3, NO_2, Ph, F-Ph, CH_3O-Ph, naphthoyl, and pyrazoyl) (chemical structure of these compounds are shown in Figure 1). The *in vitro* antibacterial and antifungal activities of the synthesized thiosemicarbazone derivatives were evaluated against *S. aureus* and *C. albicans,* while the *in vitro* cytotoxic effect of these thiosemicarbazones was studied against several human tumor cell lines. The antioxidant activity was also studied using the DPPH method. Relevant IC_{50} and MIC values obtained from biological assays are also presented in Figure 1.

2. Materials and Methods

2.1. Reagents and Instruments. All the chemicals were obtained from commercial suppliers and used as received. A Büchi melting point B-545 apparatus was employed for the determination of melting points. Infrared spectra (KBr discs) were recorded in the 4000–400 cm^{-1} region using a Nicolet iS10 FT-IR spectrometer. Mass spectra measurements of the prepared compounds in methanol solutions were performed with the assistance of the Waters–Quattro Premier XE™ tandem quadrupole and MicrOTOF Bruker Daltonics mass spectrometers. The NMR spectra were recorded at 500 or 400 or 300, 125.8 or 101 or 75.5, and 376 MHz for ^1H, ^{13}C, and ^{19}F acquisition, respectively, using dimethylsulfoxide-d_6 as solvent and tetramethylsilane

($SiMe_4$) as an internal reference, and employing the Bruker Avance III HD 500 or Varian Mercury Plus 400 or 300 spectrometers. The chemical shifts expressed in ppm (δ) values for ^1H and ^{13}C spectra were referenced to residual ^1H and ^{13}C present in deuterated dimethylsulfoxide. The NMR data are reported according to the atom numbers shown on the structural formulas for thiosemicarbazone derivatives as seen in Scheme 1.

2.2. Experimental Procedures

*2.2.1. General Procedure for the Synthesis of Compounds **1–10**.* Compounds **1–10** were prepared according to the procedure described in the literature [22].

Thiosemicarbazones were synthesized (Scheme 1) by refluxing the methanol solution (40 mL) of thiosemicarbazide (0.182 g, 2 mmol) with the furan-2-carbaldehyde derivative (2 mmol), dissolved in the same solvent (40–60 mL), for 3 h. Then, the mixture was stirred for one day at room temperature. For compounds **2**, **6**, **7**, and **8,** good quality crystals were grown in methanol by slow evaporation of the solvent from their solutions. These crystals were selected and used for single crystal X-ray diffraction studies. The other prepared compounds were obtained as solids. These products were filtered, washed with ethanol (30 mL), dried, and recrystallized from hot acetone.

*Furan-2-carbaldehyde thiosemicarbazone (**1**).* Brown solid. Yield: 90%. m.p.: 170°C. IR (KBr)ν/cm^{-1}: 3408, 3215 (NH_2); 3127 (NHCS); 1607 (C=N); 1275 (C-O); 1016 (N-N); 841 (C=S). ESI-MS, m/z: 168.773 $[M-H]^-$(calcd. for $C_6H_7N_3OS$, 169.203). 1H NMR (500 MHz, DMSO-d_6): δ (ppm) 11.41 (s, 1H, =N-N-H), 8.20 (s, 2H, NH_2), 7.97 (s, 1H, H-C=N), 7.80 (d, 1H, J = 1.8 Hz, C5 furan), 7.62 (s, 2H, NH_2), 6.96 (d, 1H, J = 3.5 Hz, C3 furan), 6.61 (dd, 1H, J = 2.0 Hz, C4 furan). ^{13}C NMR (125.76 MHz, DMSO-d_6): δ (ppm) 178.20 (-C=S), 149.87 (C2), 145.42 (C5), 132.97 (-C=N), 113.24 (C3), and 112.78 (C4).

*3-Methyl-furan-2-carbaldehyde thiosemicarbazone (**2**).* Rectangular-shaped yellow crystals. Yield: 69%. m.p.: 157-158°C. IR (KBr) ν/cm^{-1}: 3441, 3271 (NH_2); 3132 (NHCS); 1599 (C=N); 1242 (C-O); 1047 (N-N); 839 (C=S). ESI-MS, m/z: 184.054 $[M+H]^+$ (calcd. for $C_7H_9N_3OS$, 183.234). ^1H NMR (300 MHz, DMSO-d_6): δ (ppm) 11.28 (s, 1H, =N-N-H), 8.16 and 8.07 (s, 1H, H-C=N), 7.70 (d, 1H, J = 1.70 Hz, C5 furan), 7.35 (s, 2H, NH_2), 6.50 (d, 1H, J = 1.70 Hz, C4 furan), 2.15 (s, 3H, CH_3). ^{13}C NMR (75 MHz, DMSO-d_6): δ (ppm) 177.39 (-C=S), 144.79 (C5), 144.42 (C2), 132.85 (-C=N), 124.02 (C3), 114.97 (C4), and 10.16 (CH_3).

*5-Hydroxymethyl-furan-2-carbaldehyde thiosemicarbazone (**3**).* Pale yellow solid. Yield: 86%. m.p.: 185-186°C. IR (KBr) ν/cm^{-1}: 3433, 3310 (NH_2); 3119 (NHCS); 1595 (C=N); 1271 (C-O); 1059 (N-N); 851 (C=S). ESI-MS, m/z: 197.912 $[M-H]^-$ (calcd. for $C_7H_9N_3SO_2$, 199.230). ^1H NMR (500 MHz, DMSO-d_6): δ (ppm) 11.31 (s, 1H, =N-N-H), 8.19, 7.94 and 7.56 (s, 1H, H-C=N), 6.89 (d, 1H, J = 3.40 Hz, C3 furan), 6.43 (d, 1H, J = 3.40 Hz, C4 furan), 5.32 (s, 2H, NH_2), 4.42 (d, 2H, J = 5.0 Hz, -CH_2OH). ^{13}C NMR (125.76 MHz, DMSO-d_6): δ (ppm) 178.13 (-C=S), 158.22 (C2), 149.00 (C5), 133.15 (-C=N), 114.18 (C3), 109.86 (C4), and 56.21 (-CH_2OH).

*5-Trifluoromethyl-furan-2-carbaldehyde thiosemicarbazone (**4**).* Pale yellow solid. Yield: 69%. m.p.: 178°C. IR (KBr) ν/cm^{-1}: 3429, 3264 (NH_2); 3152 (NHCS); 1601 (C=N); 1308 (C-O); 1018 (N-N); 808 (C=S). ESI-MS, m/z: 235.849 $[M-H]^-$ (calcd. for $C_7H_6N_3OSF_3$, 237.200). ^1H NMR (500 MHz, DMSO-d_6): δ (ppm) 11.64 (s, 1H, =N-N-H), 8.38 (s, 2H, NH_2), 7.99 (s, 1H, H-C=N), 7.85 (s, 2H, NH_2), 7.34 (d, 1H, J = 3.7 Hz, C4 furan), 7.17 (d, 1H, J = 3.8 Hz, C3 furan). ^{13}C NMR (125.76 MHz, DMSO-d_6): δ (ppm) 178.69 (-C=S), 153.04 (C2), 141.89 (q, J = 41.3 Hz, C5), 131.24 (-C=N), 120.46 (q, J = 269.3 Hz, CF_3), 115.57 (d, J = 2.7 Hz, C4), and 112.29 (C3).

*5-Nitro-furan-2-carbaldehyde thiosemicarbazone (**5**).* Orange solid. Yield: 74%. m.p.: 227°C. IR (KBr) ν/cm^{-1}: 3458, 3296 (NH_2); 3084 (NHCS); 1591 (C=N); 1244 (C-O); 1017 (N-N); 826 (C=S). ESI-MS, m/z: 212.853 $[M-H]^-$ (calcd. for $C_6H_9N_4O_3S$, 214.202). ^1H NMR (500 MHz, DMSO-d_6): δ (ppm) 11.85 (s, 1H, =N-N-H), 8.52 and 8.02 (s, 2H, NH_2), 7.97 (s, 1H, H-C=N), 7.78 (d, 1H, J = 4.0 Hz, C4 furan), 7.37 (d, 1H, J = 4.0 Hz, C3 furan). ^{13}C NMR (125.76 MHz, DMSO-d_6): δ (ppm) 178.89 (-C=S), 153.07 (C5), 152.03 (C2), 130.24 (-C=N), 115.58 (C4), and 113.66 (C3).

*5-Phenyl-furan-2-carbaldehyde thiosemicarbazone (**6**).* Rombic-shaped beige crystals. Yield: 63%. m.p.: 214°C. IR (KBr) ν/cm^{-1}: 3402, 3235 (NH_2); 3142 (NHCS); 1599 (C=N); 1273 (C-O); 1020 (N-N); 831 (C=S). ESI-MS, m/z: 246.069 $[M+H]^+$ (calcd. for $C_{12}H_{11}N_3OS$, 245.301). 1H NMR (300 MHz, DMSO-d_6): δ (ppm) 11.49 (s, 1H, =N-N-H), 8.26 (s, 2H, NH_2), 7.98 (s, 1H, H-C=N), 7.88–7.79 (m, 2H: H2′, H6′, Ph), 7.76 (s, 2H, NH_2), 7.51–7.40 (m, 2H: H3′, H5′, Ph), 7.38–7.28 (m, 1H, H4′, Ph), 7.11 (d, 1H, J = 3.6 Hz, C4 furan), 7.07 (d, 1H, J = 3.6 Hz, C3 furan). ^{13}C NMR (76 MHz, DMSO-d_6): δ (ppm) 177.66 (-C=S), 154.50 (C5), 148.97 (C2), 131.39 (-C=N), 129.51 (C1′, Ph), 128.93 (C3′ and C5′, Ph), 128.20 (C4′, Ph), 123.98 (C2′and C6′, Ph), 115.32 (C3), 108.29 (C4).

*5-(2-Fluorophenyl)-furan-2-carbaldehyde thiosemicarbazone (**7**).* Needle-shaped beige crystals. Yied: 89%. m.p.: 208-209°C. IR (KBr) ν/cm^{-1}: 3402, 3225 (NH_2); 3136 (NHCS); 1601 (C=N); 1215 (C-O); 1024 (N-N); 816 (C=S). ESI-MS, m/z: 264.059 $[M+H]^+$ (calcd. for $C_{12}H_{10}N_3OSF$, 263.291). ^1H NMR (400 MHz, DMSO-d_6): δ (ppm) 11.53 (s, 1H, =N-N-H), 8.29 (s, 2H, NH_2), 8.00 (s, 1H, H-C=N), 8.04–7.95 (m, H6′, Ph), 7.81 (s, 2H, NH_2), 7.37–7.27 (m, 3H: H3′, H4′, H5′, Ph), 7.12 (d, 1 H, J = 3.6 Hz, C3 furan), 6.98 (t, 1H, J = 3.7 Hz, C4 furan). ^{13}C NMR (76 MHz, DMSO-d_6): δ (ppm) 177.81 (-C=S), 158.13 (d, F-C2′, J = 250.0 Hz, Ph), 157.54 (d, C5, J = 3.4 Hz), 149.14 (C2), 131.63 (-C=N), 129.84 (d, C4′, J = 8.20 Hz, Ph), 126.39 (d, C6′, J = 2.30 Hz, Ph), 125.06 (d, C5′, J = 3.40 Hz, Ph), 117.54 (d, C1′, J = 11.90 Hz, Ph), 116.22 (d, C3′, J = 20.90 Hz, Ph), 115.14 (C3), 112.94 (d, C4,

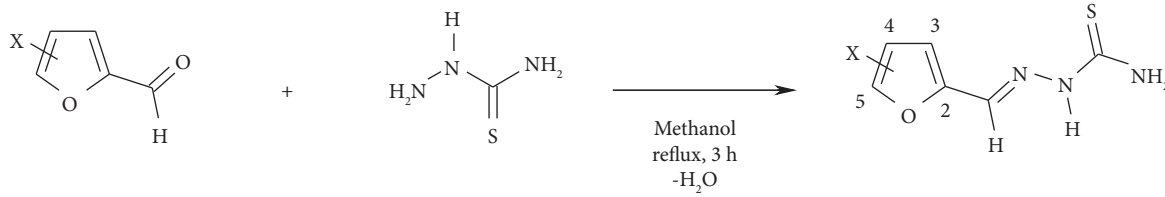

1 (X=H)
2 (X=3-CH_3)
3 (X=5-CH_2OH)
4 (X=5-CF_3)
5 (X=5-NO_2)
6 (X=5-Ph)
7 (X=5-(2′-FPh))
8 (X=5-(4′-OCH_3Ph))
9 (X=5-Naphthoyl))
10 (X=5-(1H-Pyrazoyl))

Scheme 1: Synthesis of the X-furan-2-carbaldehyde thiosemicarbazone derivatives.

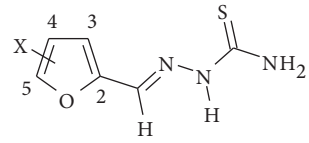

Compound	IC_{50}(uM)			MIC (*ug/mL*)	
	Tumor cell line			Gram-positive bacteria	
	HuTu80	M-14	LNCaP	*S. aureus* ATCC29213	*S. aureus* ATCC700699
5-FU	8.86	**57.73**	**11.97**	-	-
Gentamicin	-	-	-	10	**>100**
1 (X=H)	196.68	>372.34	>372.34	NA	NA
2 (X=3-CH_3)	261.96	>343.83	151.46	NA	NA
3 (X=5-CH_2OH)	116.37	>316.22	>316.22	NA	NA
4 (X=5-CF_3)	>265.60	>265.60	>265.60	NA	NA
5 (X=5-NO_2)	13.36	**27.73**	22.55	10	**1**
6 (X=5-Ph)	>256.25	>256.25	55.69	NA	NA
7 (X=5-(2′-FPh))	>239.28	>239.28	21.80	NA	NA
8 (X=5-(4′-OCH_3Ph))	53.96	206.03	13.31	NA	NA
9 (X=5-Naphthoyl))	103.36	>213.30	**7.69**	NA	NA
10 (X=5-(1H-Pyrazoyl))	>267.78	>267.78	233.52	NA	NA

Figure 1: General structure of the prepared X-furan-2-carbaldehyde thiosemicarbazone derivatives with some IC_{50} and MIC values obtained from their biological assays.

J = 7.78 Hz). ^{19}F-NMR (376 MHz, δ, ppm, DMSO-d_6): −114.39 – -114.53 (m, F-Ph).

*5-(4-Methoxyphenyl)-furan-2-carbaldehyde thiosemicarbazone (**8**)*. Rectangular-shaped orange crystals. Yield: 75%. m.p.: 203-204°C. IR (KBr) ν/cm^{-1}: 3362, 3264 (NH_2); 3171 (NHCS); 1607 (C=N); 1248 (C-O); 1030 (N-N); 829 (C=S). ESI-MS, m/z: 276.080 $[M+H]^+$ (calcd. for $C_{13}H_{13}N_3O_2S$, 275.328). ^{1}H NMR (400 MHz, DMSO-d_6): δ (ppm) 11.45 (s, 1H, =N-N-H), 8.23 (s, 2H, NH_2), 7.96 (s, 1H, H-C=N), 7.71 (s, 2H, NH_2), 7.03–6.96 (m, 2H: H3′, H5′, Ph), 7.80–7.73 (m, 2H: H2′, H6′, Ph), 7.02 (d, 1H, J = 3.6 Hz, C3 furan), 6.94 (d, 1H, J = 3.5 Hz, C4 furan), 3.79 (s, 3H, OCH_3). ^{13}C NMR (101 MHz, DMSO-d_6): δ (ppm) 177.56 (-C=S), 159.35 (C4′, Ph), 154.86 (C5), 148.21 (C2), 132.07 (-C=N), 125.64 (C2′ and C6′, Ph), 122.39 (C1′, Ph), 115.61 (C3), 114.40 (C3′ and C5′, Ph), 106.59 (C4), and 55.24 (OCH_3).

*5-(1-Naphthyl)-furan-2-carbaldehyde thiosemicarbazone (**9**)*. Beige solid. Yield: 77%. m.p.: 200°C. IR (KBr) ν/cm^{-1}: 3362, 3235 (NH_2); 3150 (NHCS); 1601 (C=N); 1248 (C-O); 1020 (N-N); 831 (C=S). ESI-MS, m/z: 293.777 $[M-H]^-$ (calcd. for $C_{16}H_{13}N_3OS$, 295.361). 1H NMR (500 MHz, DMSO-d_6): δ (ppm) 11.54 (s, ^{1}H, =N-N-H), 8.42 (d, H8′, $J = 8.4$ Hz, naphthyl), 8.27 (s, 2H, NH_2), 8.07 (s, 1H, H-C=N), 8.02 (d, H5′, $J = 8.2$ Hz, naphthyl), 7.90 (d, H2′, $J = 7.6$ Hz, naphthyl), 7.72 (s, 2H, NH_2), 7.65–7.58 (m, 4H: H3′, H4′, H6′, H7′, naphthyl), 7.22 (d, 1H, $J = 3.50$ Hz, C4 furan), 7.12 (d, 1H, $J = 3.70$ Hz, C3 furan). ^{13}C- NMR (125.76 MHz, DMSO-d_6): δ (ppm) 178.20 (C=S), 154.43 (C5), 150.00 (C2), 134.07 (C=N), 132.69, 129.70, 129.67, 129.20, 127.75, 127.36, 126.89, 126.74, 126.01, 125.33, (Naphthalene), 115.11 (C3), and 112.69 (C4).

*5-(1H-Pyrazol-5-yl)-furan-2-carbaldehyde thiosemicarbazone (**10**)*. Brown solid. Yield: 85%. m.p.: 229°C. IR (KBr) ν/cm^{-1}: 3443, 3306 (NH_2); 3136 (NHCS); 1564 (C=N); 1275 (C-O); 1015 (N-N); 829 (C=S). ESI-MS, m/z: 236.226 $[M+H]^+$ (calcd. for $C_9H_9N_5OS$, 235.266). ^{1}H NMR (500 MHz, DMSO-d_6): δ (ppm) 13.42 (br, 1H, –NH, pyrazole), 13.08 and 11.45 (s, 1H, =N-N-H), 8.24 (s, 2H, NH_2), 7.98 (s, 1H, H-C=N), 7.82 (s, H3′, Pyrazole), 7.68 (s, 2H, NH_2), 7.05 (d, 1H, $J = 3.5$ Hz, C3 furan), 6.83 (s, H4′, Pyrazole), 6.67 (d, 1H, $J = 2.8$ Hz, C4 furan). ^{13}C NMR (125.76 MHz, DMSO-d_6): δ (ppm) 178.02 (-C=S), 151.42 (C2), 148.72 (C5), 142.73 (C3′, Ph), 132.84 (-C=N), 130.27 (C5′, Ph), 115.07 (C4), 108.11 (C3), and 102.95 (C4′, Ph).

2.2.2. Single Crystal X-Ray Diffraction Studies. For compounds **2** and **7**, crystallographic data were collected at 200 K using a STOE IPDS-2T imaging plate diffractometer equipped with a sealed X-ray tube (Mo Kα radiation, $\lambda = 0.71073$ Å), while for compounds **6** and **8**, data collection was performed at 180 K with a STOE StadiVari diffractometer equipped with a microfocus X-ray tube (Cu Kα radiation, $\lambda = 1.54186$ Å) and a Dectris Pilatus 300k detector. Unit cell parameters were determined and intensity data were integrated using Stoe X-Area software [27]. A numerical absorption correction was applied, and for microsource data, also, a scaling correction was performed. The data were corrected for Lorentz and Polarization effects [27]. Direct methods were applied to solve the structures using ShelxT [28], and the structures were refined with ShelxL [29]. For all nonhydrogen atoms, anisotropic thermal parameters were used. In the structure analysis of **2,** hydrogen atoms were localized and refined with isotropic thermal parameters, and for **6**, **7** and the C-H groups in **8,** the hydrogen atoms were included on idealized positions applying the riding model. The N–H hydrogen atoms in **8** were refined with isotropic thermal parameters. Diagrams of the molecular structures were obtained using Diamond software [30]. Crystal data, experimental details, and refinement results are listed in Table 1.

2.2.3. Biological Experiments

(1) Antitumor Activity. Cytotoxicity of the synthesized thiosemicarbazone derivatives **1**–**10** and 5-fluorouracyl as reference drug was carried out on seven tumor cell lines: H460 (human lung large cell carcinoma), HuTu80 (human duodenum adenocarcinoma), DU145 (human prostate carcinoma), MCF-7 (human breast adenocarcinoma), M-14 (human amelanotic melanoma), HT-29 (human colon adenocarcinoma), and LNCaP (human prostate adenocarcinoma), as well as on the BALB/3T3 nontumor cell line. They were kindly given by the National Cancer Institute or American Type Culture Collection (ATCC). Cell viability was evaluated by the sulforhodamine B colorimetric assay [31].

The tumor cell lines were maintained in Eagle's minimal essential medium (MEM) containing 50 μg/mL gentamycin and 10% fetal bovine serum (H460, HuTu80, and DU145), and in RPMI 1640 enriched with 7.5% fetal bovine serum and 50 μg/mL gentamycin (M14, MCF-7, and HT-29). Besides, Dulbecco´s modified Eagle´s medium (DMEM) containing 10% fetal calf serum and 50 μg/mL gentamycin was used for the maintenance of the BALB/3T3 and LNCaP cell lines. Cells were grown in a humidified 5% CO_2 incubator and 95% air at 37°C.

(2) In Vitro Antitumor Assay. For a performed experiment, the cells were inoculated into 96-well plates at plating densities ranging from 3000 to 5000 cells per well and kept in humidified 5% CO_2 incubator for 24 h at 37°C, prior to the addition of the compounds. After 24 h, a plate containing the different cell lines was fixed with TCA in order to obtain the basal amount of cells. The solutions of the prepared compounds in DMSO (1.0, 4.0, 16.0, and 63.0 μg/mL) and 5-fluorouracyl in DMSO (0.20, 0.70, 2.90, and 11.70 μg/mL) were transferred to the plates containing the different cell lines and incubated for an additional 48 h at 37°C. Appropriate solvent controls were tested for comparison. After the 48 h, each plate was treated with TCA, washed, and air dried, and then it was stained with 0.4% sulforhodamine B dissolved in 1% acetic acid for 20 minutes at room temperature. After staining, unbound dye was discarded by washing with 1% acetic acid. A 10 mM Tris buffer solution (pH 10.5) was used with the purpose of extracting the protein-bound dye and then proceeded to read the absorbance at 510 nm on an automated microplate reader. The IC_{50} value corresponds to the concentration of the compound that inhibits cell growth by 50% and was determined graphically from percentage inhibition results-log concentrations curves. All compounds were tested in duplicate.

(3) Antibacterial Tests. The *in vitro* antibacterial activity of the furan-2-carbaldehyde thiosemicarbazone derivatives **1**–**10** was studied against some of Gram-positive bacteria: *Staphylococcus aureus* ATCC43300, *Staphylococcus aureus* ATCC29213, *Staphylococcus aureus* ATCC25923, and *Staphylococcus aureus* ATCC700699, using the standard microdilution method and employing M07-A8 protocols CLSI [32]. Nitrofurantoin and Gentamicin were tested and used as standard reference drugs. Briefly, inoculum was prepared with fresh bacterial cultures (suspended for 18 h) in NaCl 0.8% until to get an optical density in the range of 0.08–0.1 at 620 nm, which was diluted again at 1 : 20 with Müller–Hinton broth II (MHBII, Difco). The prepared compounds were dissolved in 100% dimethyl sulfoxide (DMSO) to obtain 50 μg/μL

Table 1: Crystallographic data of compounds **2**, **6**, **7**, and **8**.

	2	**6**	**7**	**8**
Empirical formula	$C_7H_9N_3OS$	$C_{12}H_{11}N_3OS$	$C_{12}H_{10}FN_3OS$	$C_{13}H_{13}N_3O_2S$
Formula weight	183.23	245.30	263.29	275.33
Temperature (K)	200	180	200	180
Wavelength (Å)	0.71073	1.54186	0.71073	1.54186
Crystal system	Monoclinic	Orthorhombic	Monoclinic	Triclinic
Space group	$P2_1/c$	$Pbca$	$P2_1/c$	$P\bar{1}$
a (Å)	7.2206(8)	10.1489(5)	14.9278(6)	7.2431(4)
b (Å)	8.3917(4)	27.5972(10)	8.3003(5)	8.5206(4)
c (Å)	15.3440(5)	8.5485(3)	10.1599(4)	10.8025(5)
α (°)	90	90	90	81.540(4)
β (°)	103.465(5)	90	98.088(3)	83.145(4)
γ (°)	90	90	90	78.709(4)
Volume (Å^3)	904.18(11)	2394.3(2)	1246.34(10)	643.84(6)
Z	4	8	4	2
Density (calc.) (g/cm^3)	1.346	1.361	1.403	1.420
Absorption coefficient (mm^{-1})	0.314	2.298	0.263	2.260
Crystal size (mm^3)	0.34·0.38·0.42	0.085·0.24·0.25	0.087·0.14·0.38	0.030·0.078·0.15
θ range for data collection (°)	2.7 – 28.0	6.0 – 70.9	2.7 – 27.0	4.0 – 70.0
Reflections collected	7445	22123	9404	7454
Independent reflections [R_{int}]	2177 [0.041]	2277 [0.051]	2615 [0.026]	2392 [0.022]
Data/restraints/parameters	2177/0/146	2277/0/154	2615/0/164	2392/0/186
Goodness-of-fit on F^2	1.041	1.102	1.029	1.036
R indices [$I > 2\sigma(I)$]	$R1 = 0.030$; $wR2 = 0.083$	$R1 = 0.035$; $wR2 = 0.100$	$R1 = 0.031$; $wR2 = 0.082$	$R1 = 0.028$; $wR2 = 0.076$
R indices (all data)	$R1 = 0.033$; $wR2 = 0.085$	$R1 = 0.038$; $wR2 = 0.102$	$R1 = 0.040$; $wR2 = 0.086$	$R1 = 0.032$; $wR2 = 0.078$
Largest diff. peak and hole, e.Å^{-3}	0.23; −0.24	0.24; −0.21	0.24; −0.16	0.28; −0.21
CCDC number	2235827	2235828	2235829	2235830

stock solutions and then were diluted with MHBII to get a final concentration of 12.5, 25, 50, 100, 150, and 200 μg/mL. The wells were filled with these dilutions (100 μL/well) and 10 μL of inoculum suspension. Controls of growth and contamination were added. All the tests were performed in triplicate. After incubation at 35°C for 24 h, 10 μL of tetrazolium violet 0.1% (Sigma T0138) was used as a growth indicator. These microplates were incubated again at 35°C for 4 h and the minimum inhibitory concentration (MIC) value was determined considering the lowest sample concentration (without violet precipitate) that inhibits bacterial growth.

(4) Antifungal Activity. The *in vitro* antifungal activity of the furan-2-carbaldehyde thiosemicarbazone derivatives **1**–**10** was studied against yeast strains: *Candida albicans* ATCC90028, *Candida albicans* ATCC10231 and *Candida tropicalis* ATCC750, using the standard microdilution method. The M27-2A (CLSI) protocol was applied with few modifications [32]. Amphotericin B and Nystatin (commercial suspension) were tested and used as standard reference drugs. Briefly, inoculum was prepared with fresh cultures (suspended for 18 h) in NaCl (0.8%) adjusting at 0.08–0.1 of optical density ($\lambda = 620$ nm) followed by two dilutions (1 : 20 and 1 : 50) with RPMI medium in 2% of dextrose (RPMI-D). The stock solutions of the studied compounds (50 μg/μL) were serially diluted in RPMI-D to get various final concentrations: 0.1, 0.2, 0.3, and 0.4 mg/mL. These diluted solutions were added into 96-well plates (50 μL per well) and inoculated with 50 μL of yeast inoculum prepared before. The tetrazolium salt was used as a growth. Controls of growth and contamination were prepared, and three replicates were performed. Plates were incubated at 35°C for 72 h. The MIC value was determined similarly to that for antibacterial activity.

(5) Antioxidant Activity. The antioxidant assay by DPPH radical scavenging was performed by the microdilution method [32]. Thiosemicarbazone derivatives (50 mg/L) were serially diluted with methanol to obtain various concentrations in the region 25–2000 μg/mL. Before mixing, 100 μL of each compound was dispensed inside the microplate and immediately 10 μL of a fresh solution of DPPH (10 mg/L in methanol) was added. Plates were placed for 30 minutes in dark at 25°C. Then, the absorbance values were read at 517 nm. Ascorbic acid (reference antioxidant) was used as a positive control while methanol was used a negative control. Also, three replicates for each sample were performed. The 50% antioxidant activity (IC_{50}) was calculated from the regression curve (% I vs. sample concentration) of each tested compound or ascorbic acid [32].

3. Results and Discussion

3.1. Synthesis. The condensation reaction of furan-2-carbaldehyde derivatives with thiosemicarbazide in a 1 : 1 molar ratio in methanol solution resulted in the formation of the corresponding thiosemicarbazone derivatives **1**–**10** [22, 33, 34]. This reaction condition led to good yields (63–90%) (Scheme 1).

All the novel prepared thiosemicarbazones were characterized by mass spectrometry, IR, and ^{1}H, ^{13}C, and ^{19}F NMR spectroscopy. The synthesized compounds are soluble in MeOH, CH_2Cl_2, $CHCl_3$, CH_3COCH_3, DMF, and DMSO. The mass and spectroscopic data confirmed the proposed structures and this information is given as Supplementary Material.

3.2. Spectroscopy

3.2.1. Mass Spectral Analysis. The ESI mass spectra of all thiosemicarbazone derivatives exhibited peaks corresponding to their molecular ions ($[M+H]^+$ for **2**, **6–8,** and **10** or $[M-H]^-$ for **1**, **3–5,** and **9**). These results summarized in Table 2 confirm the proposed structural formulas of the synthesized compounds.

3.2.2. FT-IR Spectral Analysis. All thiosemicarbazone derivatives (**1–10**) displayed broad bands in the 3215–3458 and 3084–3171 cm^{-1} regions, which are attributed to the $\nu(NH_2)$ and ν(NHCS) absorptions, respectively [35, 36]. The vibrations assigned to the C=N double bond appeared as strong and medium bands around 1559–1607 cm^{-1} [37]. The imino bond formation evidences the preparation of all the thiosemicarbazone derivatives (**1–10**). The less intense bands around 1059–1015 cm^{-1} were attributed to the ν(N-N) absorptions [36]. In the infrared spectra, absorption bands assigned to the SH group in the 2650–2570 cm^{-1} region were not observed in the solid state [36, 37]. However, all the thiosemicarbazone derivatives displayed medium intensity bands at 851–808 cm^{-1}, attributable to the ν(CS) absorption. These evidences indicate that in the solid state, the studied thiosemicarbazone derivatives exist in the tautomeric thione form [38–40].

3.2.3. NMR Spectral Analysis. The characterization of the thiosemicarbazone derivatives **1–10** was carried out by using ^{1}H and ^{13}C NMR spectra, recorded in DMSO-d_6 solution. The ^{1}H and ^{13}C NMR and 2D NMR spectra rendered the chemical shifts (δ), which were assigned to the corresponding groups. As referential evidence of this characterization, multinuclear (^{1}H, ^{13}C, and ^{19}F) NMR spectra for compound **7** are presented in Figures 2–4.

The ^{1}H NMR spectra of the prepared thiosemicarbazones give singlets in the δ 11.28-11.85 region assignable to the protons of the functional group = N-NH [41]. These chemical shifts are similar to those reported for other thiosemicarbazones with fragments phenyl, chromone, and pyridine, where these compounds exist in the *E* or *Z* isomeric forms [42–44]. The –CH=N protons appeared as singlets in the region δ 7.94–8.07 [41]. The furan ring protons were located at δ 6.43–7.80 [45]. The chemical shifts of the = N-NH protons were affected by the presence of the *methyl, hydroxymethyl, trifluoromethyl, nitro,* and *naphthyl* substituents on the C-2 (in **2**) and C-5 (in **3**, **4**, **5,** and **9,** respectively) carbons of the furan ring. For **2** and **3**, the signals of the C-2 and C-5 protons are shifted upfield (0.13 and 0.10 ppm, respectively), while for **4**, **5**, and **9**, the signals of the C-5 protons are shifted downfield (0.23, 0.44, and 0.13 ppm) in relation to the furan ring without substituent groups in **1** [45]. For **3**, **4**, **5**, **6**, **9,** and **10**, the signals for the aromatic furan protons were affected due to the presence of the *hydroxymethyl, trifluoromethyl, nitro, phenyl, naphthyl,* and *pyrazoyl* substituents at the C-5 carbon of the furan ring. These protons are shifted, compared to the unsubstituted furan moiety, 0.18 ppm upfield in the position C-4 for **3** and also showed a shift to downfield for the C-3 (0.21, 0.41 and 0.16 ppm for **4**, **5,** and **9**, respectively) and C-4 (0.73, 1.17, 0.5, 0.61 and 0.22 ppm for **4**, **5**, **6**, **9,** and **10**, respectively) positions. Moreover, the signals for the phenyl ring protons were affected due to the presence of the *fluoro* and *methoxy* substituents (in **7** and **8**, respectively). These signals are shifted, in relation to the unsubstituted phenyl group in **6,** 0.16 ppm upfield for the proton at the C3′carbon (for **7**) and 0.46 ppm downfield for the protons at the C3′and C5′carbons (for **8**).

The $-NH_2$ protons in compounds **1–10** show two broad singlets at δ 7.35–8.52, due to the delocalization of electron density on the C-N bond [20, 35].

In the ^{13}C NMR spectra of the synthesized thiosemicarbazones **1–10**, the signal at δ 130.24–134.07 corresponds to the imine carbon (C=N). These chemical shifts are similar to those found for the pyrazole and pyridine thiosemicarbazone derivatives [4, 22]. The signals due to the thiocarbonyl group (C=S) for all the synthesized compounds appear in the δ 177.39–178.89 region [4, 46]. The carbon chemical shifts found on the furan ring were observed at δ 108.11–157.54 [45]. The presence of the different substituents groups on the furan ring produce slight changes in the chemical shifts of these aromatic carbons. For **5**, the electron withdrawing effect of the NO_2 group was confirmed by the downfield chemical shifts observed for C-1 (2.16 ppm), C-4 (2.80 ppm), and C-5 (7.65 ppm) of the furan ring with respect to the unsubstituted furan fragment. For **7** and **8**, the phenyl ring carbon signals were affected due to the presence of the *fluoro* and *methoxy* substituents at the C-2 and C-4 carbons, respectively. These signals are shifted at δ 11.97–12.71 and δ 14.53 upfield at the C1′, C3′ and C3′, C5′ carbons for **7** and **8**, respectively, compared to the unsubstituted phenyl fragment present in **6** [4].

On the other hand, the presence of the 2-fluorophenyl group in **7** was detected by using the ^{19}F NMR spectrum (Figure 4). A multiplet observed at δ −114.46 was due to the coupling of the fluorine atom with the aromatic protons. This chemical shift is in agreement with that found for 6-(4-fluorophenyl)-pyridine-3-carbaldehyde thiosemicarbazone (δ −114.54) [22].

3.3. X-Ray Diffraction Studies of 2, 6, 7 and 8. Crystals of **2**, **6**, **7,** and **8** suitable for single crystal structure analyses were grown in methanol by slow evaporation at room temperature from their respective concentrated methanol solutions. For the other thiosemicarbazone derivatives, except **1**, only solids were obtained from acetone. Crystal data, data collection, and refinement details are summarized in Table 1. Besides, selected bond distances and bond/torsion angles are

Table 2: Experimental values of fragment ions (m/z) found in ESI-MS spectra for thiosemicarbazone derivatives **1**–**10**.

Compounds	Molecular formula	Exact mass (g/mol)	Fragment ions (m/z)
1	$C_6H_7N_3OS$	169.203	168.773 $[M-H]^-$
2	$C_7H_9N_3OS$	183.234	184.054 $[M+H]^+$
3	$C_7H_9N_3SO_2$	199.230	197.912 $[M-H]^-$
4	$C_7H_6N_3OSF_3$	237.200	235.849 $[M-H]^-$
5	$C_6H_6N_4O_3S$	214.202	212.853 $[M-H]^-$
6	$C_{12}H_{11}N_3OS$	245.301	246.069 $[M+H]^+$
7	$C_{12}H_{10}N_3OSF$	263.291	264.059 $[M+H]^+$
8	$C_{13}H_{13}N_3O_2S$	275.328	276.080 $[M+H]^+$
9	$C_{16}H_{13}N_3OS$	295.361	293.777 $[M-H]^-$
10	$C_9H_9N_5OS$	235.266	236.226 $[M+H]^+$

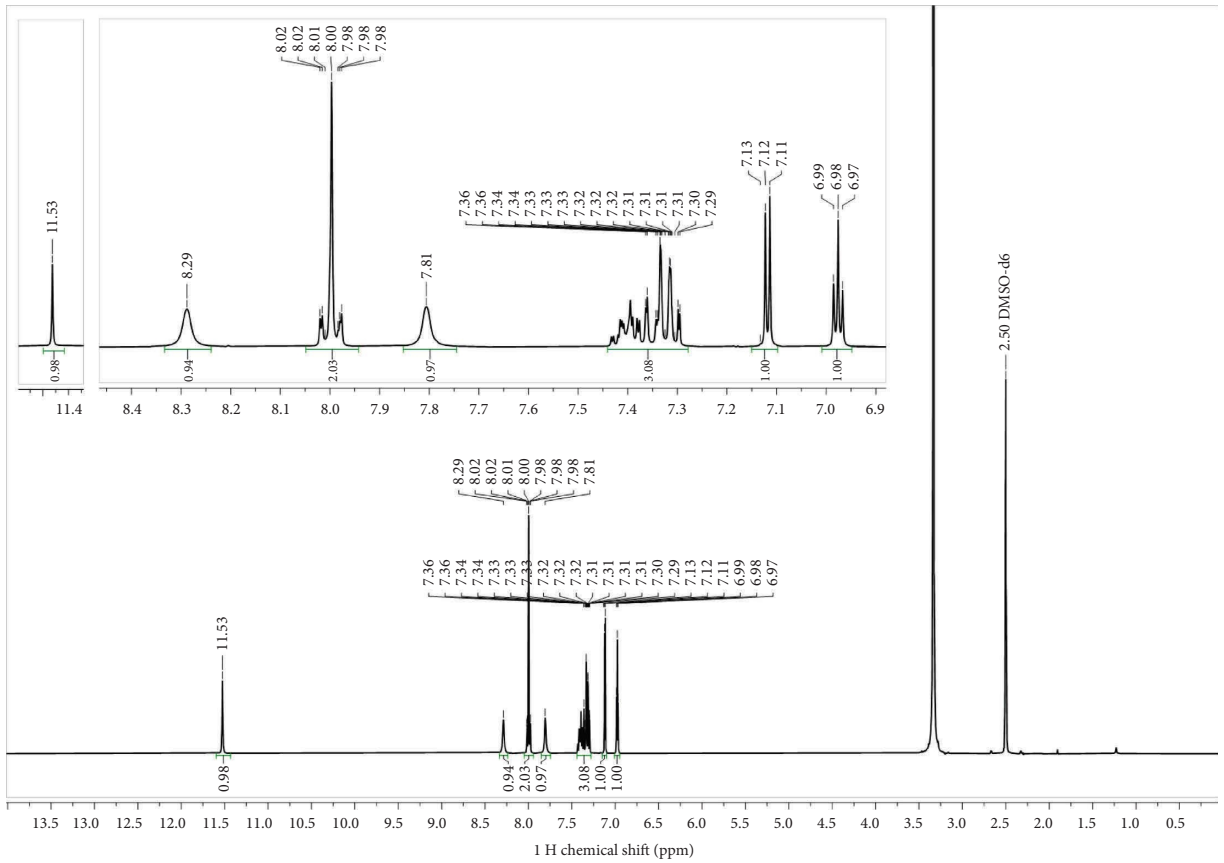

Figure 2: ^{1}H NMR spectrum of compound **7**.

given in Tables 3 and 4, respectively. Hydrogen-bonding interactions for **2, 6, 7,** and **8** are summarized in Table 5. The ORTEP diagrams of compounds **2**, **6**, **7,** and **8** are shown in Figures 5–8.

As reported in Table 1, **2** and **7** belong to the monoclinic system, space group $P2_1/c$, while **6** crystallizes in the orthorhombic space group *Pbca* and **8** in the triclinic space group $P\bar{1}$, with one molecule in each asymmetric unit.

All crystal structures show that the thiosemicarbazone unit binds in the 2-position to the furan ring via the C atom of the C=N double bond. Packing of the molecules in the crystal and structural details depend on the other substituents of the furan group. The ORTEP diagrams (Figures 5–7) reveal that **2**, **6,** and **7** exist in the *E* conformation regarding the substituents at the N1-C6 and N1-C11 bond, respectively. The torsion angles C5-C6-N1-N2 in **2** (–179.5(1)°) and C10-C11-N1-N2 in **6** and **7** (175.6(1) and 175.0(1)°) confirm the coplanar arrangement with *E* conformation. In contrast, the corresponding bond N1-C12 in **8** (Figure 8) exhibits *Z* conformation with an torsion angle C11-C12-N1-N2 of −1.3(2)°. This allows an intramolecular hydrogen bond (Figure 8) involving the furan ring oxygen atom O2 and –N1-N2-H hydrogen with an O2. . .H distance of 2.10(2) Å and O. . .H-N angle of 128(2)° (Table 5). *E* and *Z* conformations have been also observed in other thiosemicarbazone derivatives [14, 17, 40, 42, 47].

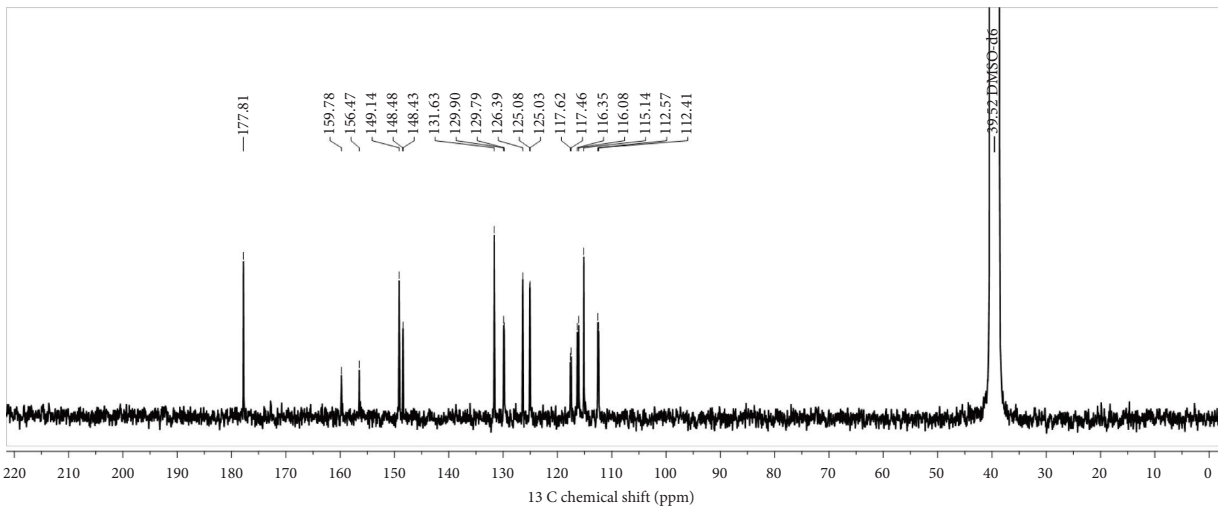

Figure 3: $^{13}C\{^{1}H\}$ NMR spectrum of compound **7**.

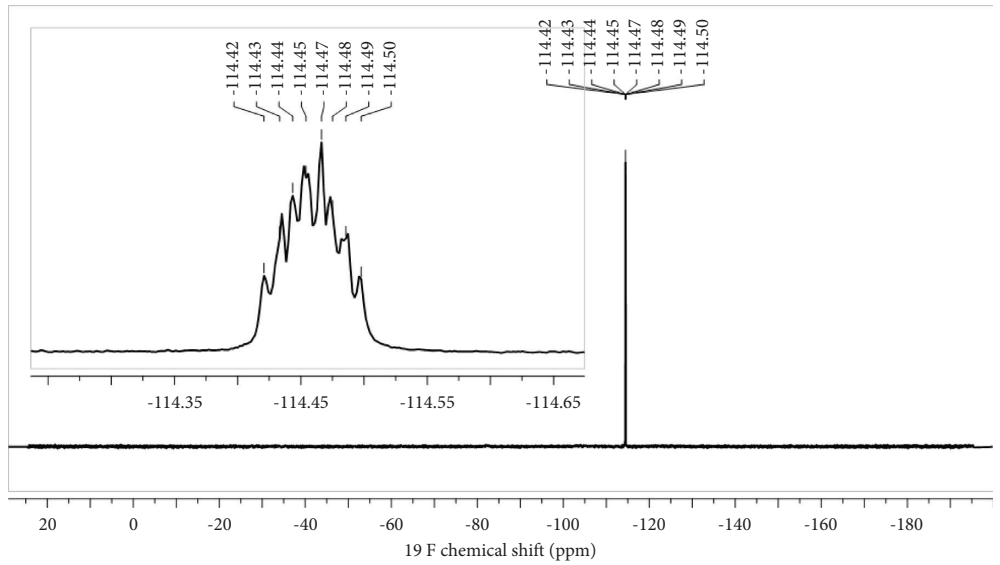

Figure 4: ^{19}F NMR spectrum of compound **7**.

Table 3: Selected bond lengths (Å) for compounds **2**, **6**, **7,** and **8**.

2		**6**		**7**		**8**	
N(1)-N(2)	1.380(1)	N(1)-N(2)	1.376(2)	N(1)-N(2)	1.382(2)	N(1)-N(2)	1.378(2)
C(6)-N(1)	1.288(1)	C(11)-N(1)	1.282(2)	C(11)-N(1)	1.284(2)	C(12)-N(1)	1.285(2)
C(7)-N(2)	1.344(1)	C(12)-N(2)	1.345(2)	C(12)-N(2)	1.343(2)	C(13)-N(2)	1.349(2)
C(7)-S(1)	1.694(1)	C(12)-S(1)	1.697(1)	C(12)-S(1)	1.698(1)	C(13)-S(1)	1.693(1)
C(7)-N(3)	1.327(2)	C(12)-N(3)	1.324(2)	C(12)-N(3)	1.325(2)	C(13)-N(3)	1.321(2)
C(1)-C(2)	1.335(2)	C(7)-C(8)	1.355(2)	C(7)-C(8)	1.359(2)	C(8)-C(9)	1.360(2)
C(3)-C(5)	1.365(2)	C(9)-C(10)	1.357(2)	C(9)-C(10)	1.355(2)	C(10)-C(11)	1.359(2)
C(5)-O(1)	1.376(1)	C(10)-O(1)	1.373(2)	C(10)-O(1)	1.366(2)	C(11)-O(2)	1.380(2)
C(5)-C(6)	1.431(2)	C(10)-C(11)	1.438(2)	C(10)-C(11)	1.439(2)	C(11)-C(12)	1.434(2)
C(3)-C(4)	1.491(2)	C(4)-C(5)	1.380(2)	C(1)-C(6)	1.391(2)	C(1)-C(6)	1.391(2)
		C(2)-C(3)	1.377(2)	C(1)-C(2)	1.370(2)	C(1)-C(2)	1.391(2)
		C(1)-C(6)	1.396(2)	C(3)-C(4)	1.381(2)	C(3)-C(4)	1.397(2)
				C(5)-C(6)	1.401(2)	C(5)-C(6)	1.403(2)
				C(1)-F(1)	1.360(2)	C(3)-O(1)	1.364(2)

Table 4: Selected bond angles and torsion angles (°) for compounds **2**, **6**, **7**, and **8**.

2		**6**		**7**		**8**	
C(5)-C(6)-N(1)	122.3(1)	C(10)-C(11)-N(1)	121.8(1)	C(10)-C(11)-N(1)	121.1(1)	C(11)-C(12)-N(1)	132.3(1)
C(7)-N(2)-N(1)	120.82(9)	C(12)-N(2)-N(1)	119.6(1)	C(12)-N(2)-N(1)	119.4(1)	C(13)-N(2)-N(1)	120.4(1)
N(2)-C(7)-S(1)	119.62(8)	N(2)-C(12)-S(1)	119.3(1)	N(2)-C(12)-S(1)	119.1(1)	N(2)-C(13)-S(1)	118.3(1)
C(6)-N(1)-N(2)	113.87(9)	C(11)-N(1)-N(2)	114.6(1)	C(11)-N(1)-N(2)	115.0(1)	C(12)-N(1)-N(2)	117.4(1)
N(3)-C(7)-S(1)	122.46(9)	N(3)-C(12)-S(1)	122.9(1)	N(3)-C(12)-S(1)	123.2(1)	N(3)-C(13)-S(1)	124.2(1)
C(1)-O(1)-C(5)	105.67(9)	C(7)-O(1)-C(10)	106.3(1)	C(7)-O(1)-C(10)	106.7(1)	C(8)-O(2)-C(11)	106.9(1)
C(2)-C(1)-O(1)	110.8(1)	C(8)-C(7)-O(1)	109.9(1)	C(8)-C(7)-O(1)	109.5(1)	C(9)-C(8)-O(2)	109.2(1)
C(3)-C(5)-C(6)	131.3(1)	C(9)-C(10)-C(11)	130.6(1)	C(9)-C(10)-C(11)	131.0(1)	C(10)-C(11)-C(12)	129.4(1)
C(6)-C(5)-O(1)	118.03(9)	C(11)- C(10)-O(1)	119.0(1)	C(11)-C(10)-O(1)	118.7(1)	C(12)-C(11)-O(2)	120.9(1)
C(3)-C(5)-O(1)	110.7(1)	C(9)-C(10)-O(1)	110.3(1)	C(9)-C(10)-O(1)	110.2(1)	C(10)-C(11)-O(2)	109.7(1)
C(2)-C(3)-C(4)	126.7(1)	C(1)-C(6)-C(7)	120.9(1)	C(5)-C(6)-C(7)	121.3(1)	C(4)-C(3)-O(1)	115.4(1)
C(4)-C(3)-C(5)	128.0(1)	C(2)-C(3)-C(4) C(2)-C(1)-C(6)	119.7(2) 120.1(1)	C(6)-C(1)-F(1) C(2)-C(3)-C(4)	118.1(1) 119.8(2)	C(2)-C(1)-C(6)	121.3(1)
C(3)-C(5)-C(6)-N(1)	−177.6(1)	C(9)-C(10)-C(11)-N(1)	−173.3(1)	C(9)-C(10)-C(11)-N(1)	−173.2(1)	C(10)-C(11)-C(12)-N(1)	−178.0(2)
C(5)-C(6)-N(1)-N(2)	−179.5(1)	C(10)-C(11)-N(1)-N(2)	175.6(1)	C(10)-C(11)-N(1)-N(2)	175.0(1)	C(11)-C(12)-N(1)-N(2)	−1.3(2)
S(1)-C(7)-N(2)-N(1)	−172.73(8)	S(1)-C(12)-N(2)-N(1)	171.07(9)	S(1)-C(12)-N(2)-N(1)	170.20(9)	S(1)-C(13)-N(2)-N(1)	176.69(9)
N(3)-C(7)-N(2)-N(1)	6.4(2)	N(3)-C(12)-N(2)-N(1)	−8.1(2)	N(3)-C(12)-N(2)-N(1)	−8.1(2)	N(3)-C(13)-N(2)-N(1)	−4.2(2)
O(1)-C(1)-C(2)-C(3)	−0.1(2)	O(1)-C(7)-C(8)-C(9)	−0.7(2)	O(1)-C(7)-C(8)-C(9)	−0.9(2)	O(2)-C(8)-C(9)-C(10)	−0.4(2)
O(1)-C(5)-C(6)-N(1)	1.6(2)	O(1)-C(10)-C(11)-N(1)	2.0(2)	F(1)-C(1)-C(6)-C(7)	1.6(2)	O(1)-C(3)-C(4)-C(5)	179.6(1)
C(4)-C(3)-C(5)-O(1)	−177.5(1)	C(2)-C(1)-C(6)-C(7)	171.5(1)	C(4)-C(5)-C(6)-C(7)	176.3(2)	C(2)-C(1)-C(6)-C(8)	−178.6(1)

Table 5: Hydrogen bonds in X-ray structures for compounds **2**, **6**, **7**, and **8**.

Compounds	D-H...A	d(D-H), Å	d(H...A), Å	d(D...A), Å	<(DHA), deg.
2	C6-H6...S1^{i}	1.00(2)	2.83(2)	3.700(1)	147(1)
	N2-H2...S1^{i}	0.86(2)	2.56(2)	3.393(1)	165(1)
	N3-H3A...S1^{ii}	0.86(2)	2.64(2)	3.379(1)	144(2)
	N3-H3B...O1^{iii}	0.85(2)	2.31(2)	2.975(1)	136(2)
	i = $-x+1$, $-y$, $-z+1$; ii = $-x+1$, $y+1/2$, $-z+3/2$, iii = $-x+1$, $y-1/2$, $-z+3/2$				
6	N2-H2A...S1^{i}	0.88	2.63	3.459(1)	158.2
	N3-H3A...S1^{ii}	0.88	3.00	3.457(1)	114.1
	N3-H3B...S1^{iii}	0.88	2.53	3.396(1)	167.9
	i = $-x+3/2$, $-y+1$, $z+1/2$; ii = $x-1/2$, y, $-z+1/2$; iii = $-x+3/2$, $-y+1$, $z-1/2$				
7	C11-H11...S1^{i}	0.95	3.02	3.837(1)	144.3
	N2-H2...S1^{i}	0.88	2.51	3.366(1)	163.1
	N3-H3B...S1^{ii}	0.88	2.52	3.366(1)	162.7
	i = $-x+1$, $y-1/2$, $-z+3/2$; ii = $-x+1$, $y+1/2$, $-z+3/2$				
8	C4-H4...O1^{i}	0.95	2.54	3.490(2)	176
	C12-H12...S1^{ii}	0.95	2.81	3.708(1)	157.4
	N2-H2...O2	0.89(2)	2.10(2)	2.743(1)	128(2)
	N3-H3A...N1^{iii}	0.86(2)	2.45(2)	3.200(2)	146(2)
	N3-H3B...S1^{iv}	0.86(2)	2.61(2)	3.451(1)	167(2)
	i = $-x$, $-y+1$, $-z$; ii = x, $y+1$, z; iii = $-x+1$, $-y+1$, $-z+2$; iv = $-x+1$, $-y$, $-z+2$				

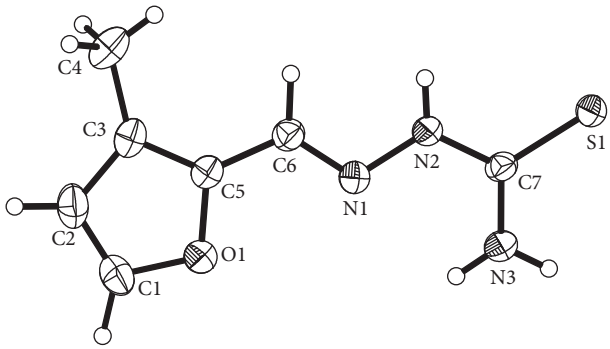

Figure 5: ORTEP diagram of **2** with thermal ellipsoids at 50% probability level.

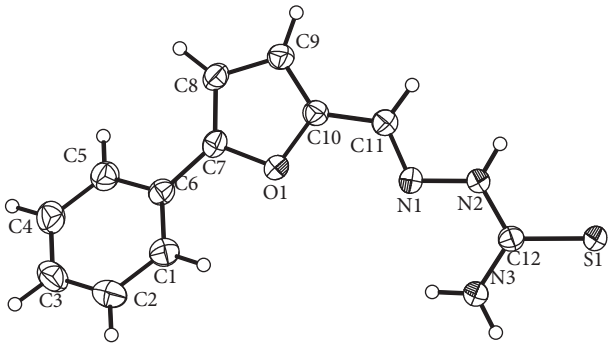

Figure 6: ORTEP diagram of **6** with thermal ellipsoids at 50% probability level.

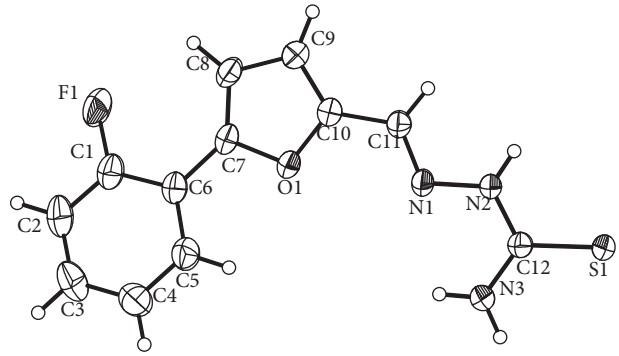

Figure 7: ORTEP diagram of **7** with thermal ellipsoids at 50% probability level.

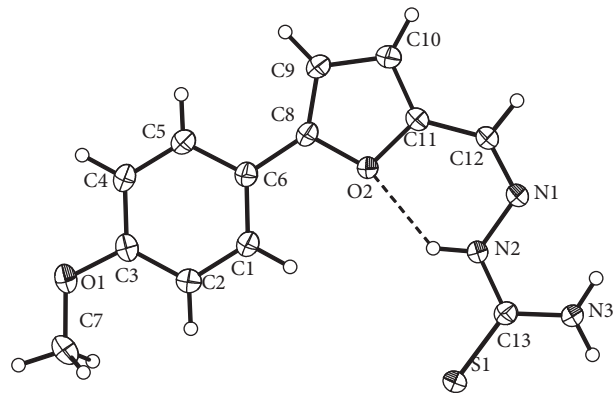

Figure 8: ORTEP diagram of **8** with thermal ellipsoids at 50% probability level.

The C=N and C=S bond lengths of 1.288(1) and 1.694(1) Å (for C6-N1 and C7-S1) in **2**, 1.282(2) and 1.697(1) Å (for C11-N1 and C12-S1) in **6**, 1.284(2) and 1.698(1) Å (for C11-N1 and C12-S1) in **7**, and 1.285(2) and 1.693(1) Å (for C12-N1 and C13-S1) in **8** are very close to the values found for 2-acetylpyrazine-N(4)-phenylthiosemicarbazone (1.285(3) and 1.671(2) Å) [24] and 2-formylpyridine-N(4)-allylthiosemicarbazone (1.280(6) and 1.673(5) Å) [48]. Besides, the C=N and C=S bond lengths found in this study are very close

to the established values for these functional groups [40]. In agreement with IR spectroscopy data, these results indicate that compounds **2**, **6**, **7,** and **8** adopt the tautomeric thione form in the solid state. Moreover, the bond distances N1-N2 (1.382–1.376 Å), N2-C (1.349–1.343 Å), and C-N3 (1.327–1.321 Å) correspond to intermediate values of distance lengths between formal single and double bonds. This evidence confirms an extensive delocalization of the electron density over the N1-N2-C-N3 chain [49].

In close approximation, the thiosemicarbazone groups can be regarded as planar evidenced by the obtained values of the maximum deviations from the least square planes of the thiosemicarbazone groups (Table S1, supplementary material). The maximum deviation is observed for C10 (0.1345(8) Å) in **7**. This planarity, with a slight deviation, is confirmed by the C-C-N1, C-N1-N2, N2-C-S1, and N3-C-S1 angles of 132.3(1)–121.1(1), 117.4(1)–113.87(9), 119.62(8)–118.3(1), and 124.2(1)–122.46(9)°, respectively, indicating the sp^2 character of the involved atoms [50]. Besides, this evidence is supported by the torsion angles C5-C6-N1-N2/S1-C7-N2-N1, C10-C11-N1-N2/S1-C12-N2-N1, C10-C11-N1-N2/S1-C12-N2-N1, and C11-C12-N1-N2/S1-C13-N2-N1 of −179.5(1)/-172.73(8), 175.6(1)/171.07(9), 175.0(1)/170.20(9), and −1.3(2)/176.69(9)° found for **2**, **6**, **7,** and **8**, respectively. These results are in agreement with the planarity of the thiosemicarbazone group which was also evidenced for 2-acetylpyrazine-N(4)-phenyl thiosemicarbazone (torsion angle N2-N3-C9-N5 of 7.3(2)°) [24] and 5-iodo-pyridine-3-carbaldehyde thiosemicarbazone (torsion angles C3-C7-N2-N3: 179.8(3)° and N2-N3-C8-N4: 4.1(6)/4.3(5)°) [22].

The dihedral angles between the thiosemicarbazone group and the furan ring as well as between the furan and the phenyl groups are also presented in Table S1 as supplementary material. In the crystal structure of **6**, the phenyl group is not coplanar with the furan ring, as evidenced by the dihedral angle of 2.56(8)° and by the torsion angles C1-C6-C7-O1: 25.1(2) and C1-C6-C7-C8: −148.4(2)°. However, for **7** and **8** the presence of the *fluoro* and *methoxy* substituent groups attached to the C2′ and C4′ carbons of the phenyl fragment cause a certain coplanarity with the furan ring, being demonstrated by the dihedral angles of 13.53(9)° in **7** and 3.47(6)° in **8** (Table S1, supplementary material) as well as by the torsion angles C1-C6-C7-O1: 172.6(1) and C5-C6-C7-O1: 10.6(2)° for **7**, and C1-C6-C8-O2: −3.6(2) and C5-C6-C8-O2: 177.2(1)° for **8**. In all studied crystal structures, the furan ring is coplanar with the thiosemicarbazone fragment within a deviation of ±11°. This evidence is confirmed by the torsion angles O1-C5-C6-N1: 1.6(2) for **2**, O1-C10-C11-N1: 2.0(2)° for **6**, O1-C10-C11-N1: 2.1(2) ° for **7** and C1-C6-C8-O2: −3.6(2)° for **8**.

The packing diagram of compound **2** (Figure 9) reveals that two parallel molecules, related by inversion symmetry, located in the central part of the unit cell and ten molecules located around the cell are stabilized by intermolecular N-H. . .O and N-H. . .S hydrogen bonds (Table 5).

The molecular packing of compounds **6** and **7** (Figures 10 and 11, respectively) reveals that a number of weak intermolecular hydrogen bonds (Table 5) occur between N2-H and S1 (for **6**: 2.63 Å, 158.2°; for **7**: 2.51 Å, 163.1°), N3-H and S1 (for **6**: 2.53/3.00 Å, 167.9/114.1°; for **7**: 2.52 Å, 162.7°), and C11-H and S1 (for **7**: 3.02, 144.3°). The intermolecular N-H. . .S hydrogen bonds connect each molecule of **6** with three neighbors, each molecule of **7** with two neighbors.

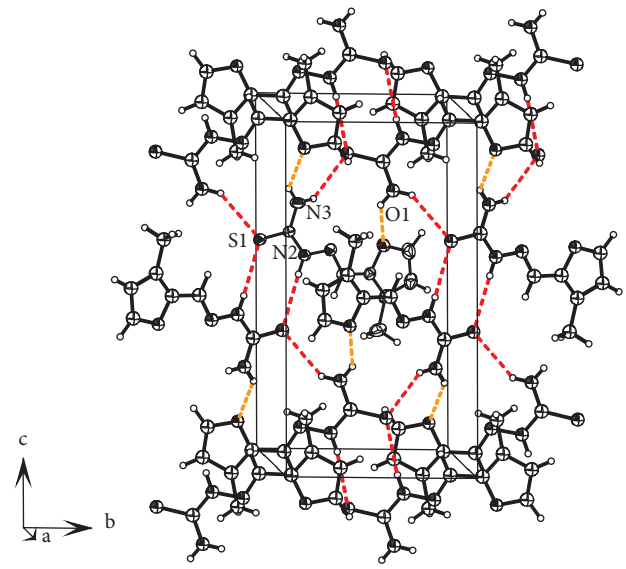

Figure 9: Packing diagram of compound **2**: Dashed lines show hydrogen bonds N-H. . .O (orange) and N-H. . .S (red).

On the other hand, the unit cell of **8** contains two molecules parallel to each other, related by inversion symmetry. For clarity, only one of them is shown in Figure 12. The diagram of compound **8** shows that a molecule inside the unit cell and two molecules located on the same side of the outer part of the cell are stabilized by intermolecular N3-H. . .N1 and N3-H. . .S1 hydrogen bonds (Table 5). Besides, neighboring molecules outside the cell are linked by intermolecular N3-H. . .S1 hydrogen bonds. Figure 13 shows that molecules of **8** are packed as layers where it is evidenced by the closest distance between atoms of neighbouring layers: C2 (phenyl group) of one layer has a distance of 3.351(2) Å to the furan ring O atom (O2) of the next layer.

For compounds **2**, **6,** and **7,** there are some intermolecular contacts that help to stabilize the molecules of these compounds such us O1. . .N3 (2.974 Å), C5(furan). . . C5(furan) (3.347 Å) and C6. . .C2(furan) (3.327 Å) for **2**, O1. . .H2C2(phenyl) (2.673 Å), N3. . .H1-C1 (2.632 Å) and C8. . .C11 (3.323 Å) for **6**, and C11. . .C8(furan) (3.350 Å), C3-H. . .F1 (2.670 Å) and C9 (furan). . .C1(phenyl) (3.265 Å) for **7**.

3.4. Biological Activity

3.4.1. In Vitro Antitumor Evaluation. The cytotoxicity of all the studied compounds **1–10** in were assayed for their antiproliferative activities *in vitro* against different human tumor cells: H460, DU145, HuTu80, MCF-7, M-14, HT-29, and LNCap, as well as these prepared compounds were

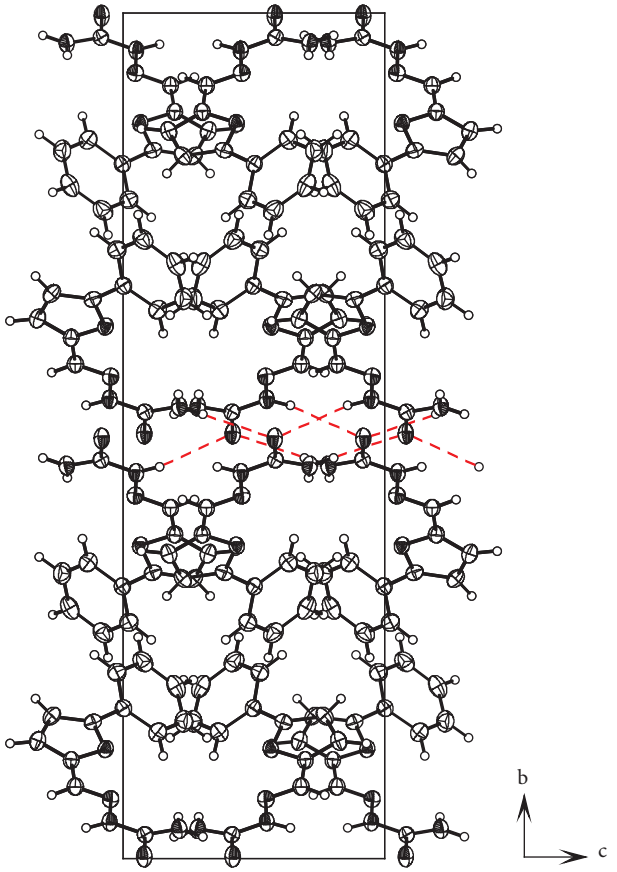

Figure 10: Packing diagram of **6** showing N-H. . .S hydrogen bonds (red). There are no intermolecular N-H. . .N bonds.

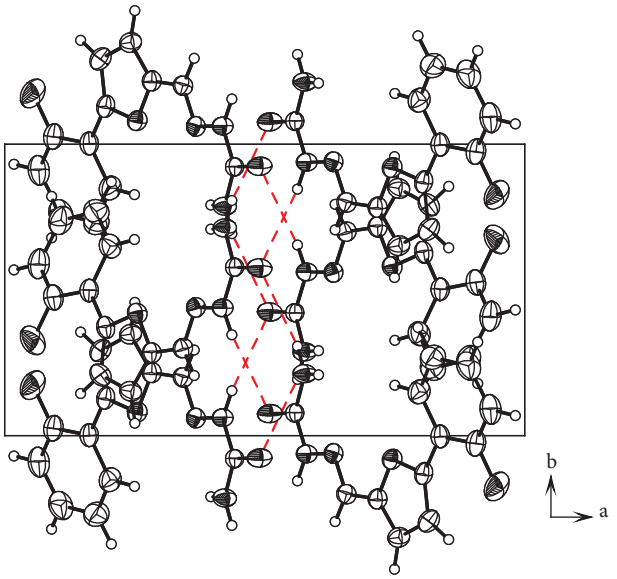

Figure 11: Packing diagram of **7** showing N-H. . .S hydrogen bonds (red).

evaluated against BALB/3T3 normal cells using the sulforhodamine B colorimetric method [31]. The 5-fluorouracile (5-FU) reference drug was assayed as positive control. The results are summarized as IC_{50} values in μM in Table 6.

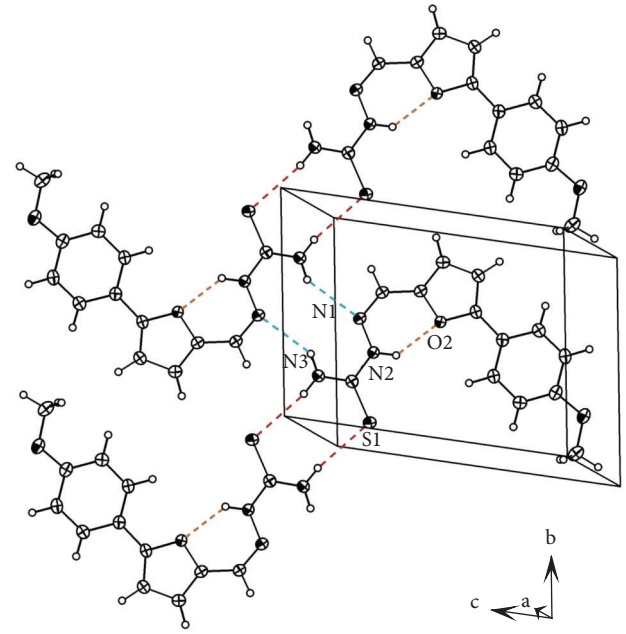

Figure 12: Diagram of compound **8** showing one layer of molecules and hydrogen bonds. Dashed lines show hydrogen bonds *intra*molecular N-H. . .O (orange), *inter*molecular N-H. . .N (blue), and N-H. . .S (red).

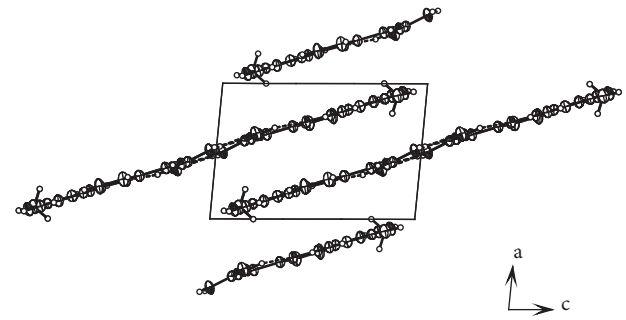

Figure 13: Packing diagram of **8**. All hydrogen bonds are within the layers.

The obtained results indicate that **5** ($X = 5\text{-}NO_2$) showed the greatest cytotoxic effect ($IC_{50} = 13.36–23.98\,\mu M$) in relation to the other tested compounds ($IC_{50} = 34.84 > 372.34\,\mu M$) against all cell lines assayed, except for the prostate carcinoma cell line (LNCaP), where **9** showed an excellent antiproliferative activity with IC_{50} value of $7.69\,\mu M$ against these cells. These results evidence that the cytotoxicity of **5** and **9** is enhanced when the *nitro* and *naphthoyl* substituent groups are attached to the furan ring at C-5 position, respectively [50, 51]. With respect to compound **5**, the effect of the *nitro* group in the increase of the antiproliferative activity is probably related to the generation of morphological cell changes associated with apoptosis [52]. Although it was shown that compound **5** exerted a great cytotoxic effect against several tested tumor cell lines, **5** showed a moderate toxicity ($IC_{50} = 11.67\,\mu M$) than 5-fluorouracile ($IC_{50} = 7.21\,\mu M$) against the 3T3 normal cells.

Table 6: *In vitro* antiproliferative activity (IC_{50} values[a] in μM) of the furan-2-carbaldehyde thiosemicarbazone derivatives (**1**–**10**) against the 3T3 nontumor cells and the different human tumor cell lines.

Comp.	3T3[b]	H460	HuTu80	DU145	MCF-7	M-14	HT-29	LNCaP
5-FU[c]	7.21 ± 1.52	8.43 ± 0.01	8.86 ± 0.97	8.39 ± 4.03	7.22 ± 1.12	**57.73 ± 23.21**	9.22 ± 0.33	**11.97 ± 0.89**
1	>372.34	>372.34	196.68 ± 16.09	>372.34	366.43 ± 6.11	>372.34	>372.34	>372.34
2	>343.83	>343.83	261.96 ± 81.87	>343.83	>343.83	>343.83	>343.83	151.46 ± 21.14
3	286.10 ± 5.0	>316.22	116.37 ± 3.72	>316.22	>316.22	>316.22	>316.22	>316.22
4	>265.6	>265.6	>265.6	>265.6	>265.6	>265.6	>265.6	>265.6
5	11.67 ± 2.33	16.62 ± 0.35	13.36 ± 0.05	23.98 ± 1.34	17.43 ± 0.03	**27.73 ± 3.34**	15.91 ± 0.53	22.55 ± 0.17
6	>256.25	>256.25	>256.25	>256.25	>256.25	>256.25	>256.25	55.69 ± 7.15
7	>239.28	>239.28	>239.28	>239.28	>239.28	>239.28	>239.28	21.80 ± 0.59
8	75.35 ± 14.20	203.85 ± 6.81	53.96 ± 5.59	225.19 ± 3.63	107.36 ± 16.65	206.03 ± 4.63	120.27 ± 9.44	13.31 ± 2.14
9	190.95 ± 22.36	>213.30	103.36 ± 68.89	184.28 ± 29.02	34.84 ± 4.73	>213.30	>213.30	**7.69 ± 0.21**
10	>267.78	255.03 ± 4.25	>267.78	>267.78	>267.78	>267.78	>267.78	233.52 ± 33.69

[a]IC_{50}: Concentration of the compound (μM) that causes a 50% cell growth inhibition after 48 h of compound exposure. The IC_{50} values are averages of two independent assays. The values are mean ± standard deviation of two independent experiments. [b]Mouse embryonic fibroblast cells. [c]5-fluorouracile. Bold values represent a comparison of the best obtained results of the tested compounds with those obtained for the antitumoral drug for clinical use, 5-FU.

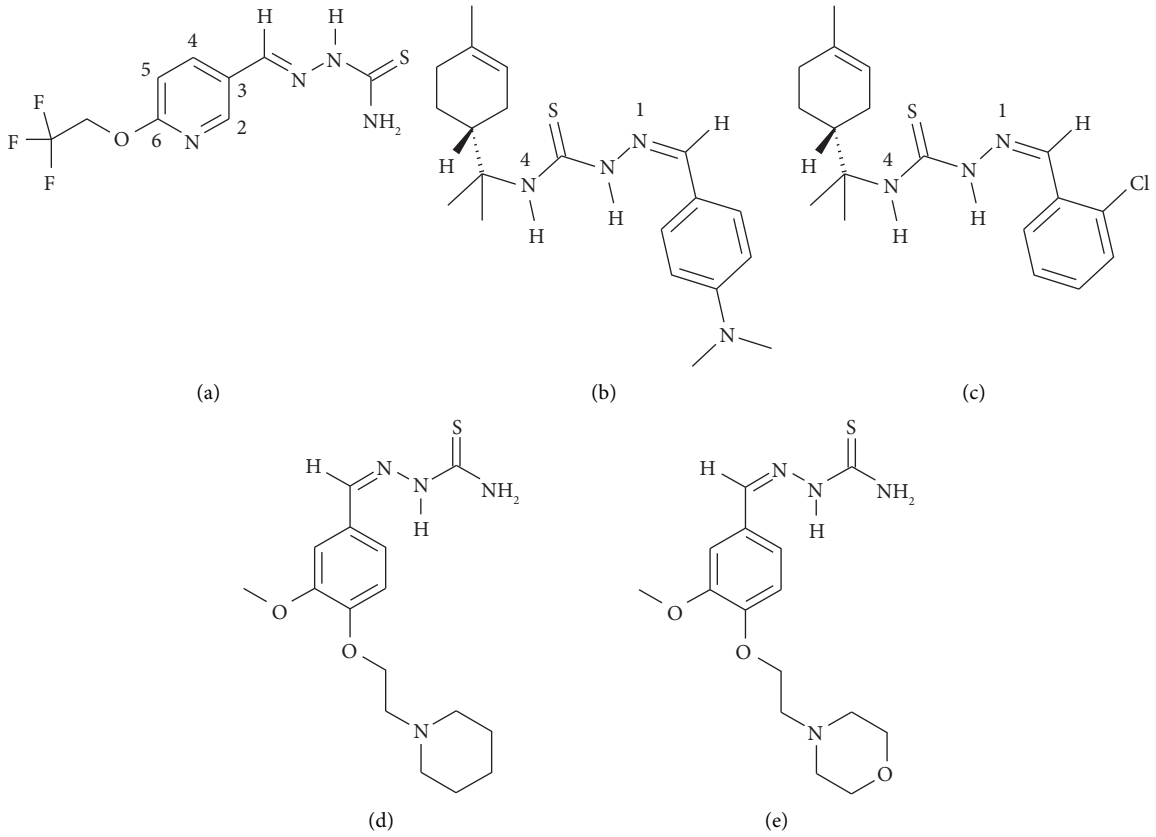

Figure 14: Structures of the comparative thiosemicarbazone derivatives I (a–e).

On the other hand, substituting the hydrogen atom at the C-5 of the furan ring with the 4-methoxyphenyl group increased the cytotoxicity of **8** ($IC_{50} = 13.31\ \mu M$) in comparison to the other tested thiosemicarbazones, except for **9** against the LNCaP cell line. With respect to the 5-fluorouracil (5-FU) antitumor drug ($IC_{50} = 11.97\ \mu M$) assayed against LNCaP cell line, **8** exhibited similar cytotoxic activiy.

Compound **5** was 1.9, 2.8, and 8.3 times less cytotoxic than 6-(1-trifluoroethoxy)pyridine-3-carbaldehyde thiosemicarbazone (Figure 14(a)) assayed against HuTu80, MCF-7, and M-14 cells [22]. These results indicate that the 6-(1-trifluoroethoxy)pyridinyl group bound to the thiosemicarbazone fragment exerted a greater antiproliferative effect than the 5-nitrofuran group. However, **5** assayed against H460 and HT-29 cells was more cytotoxic than compounds (+)-(R)-N(1)-{[4-(dimethylamino)-phenyl]-methylene}- N(4)-[2–(4-methylcyclohex-3-en-1-yl)-propan-2-yl]- thiosemicarbazide (Figure 14(b)) and (+)-(R)-N(1)-[(2-chlorophenyl)-methylene]-N(4)-[2–(4- methylcyclohex-3-en-1-yl)-propan-2-yl]-thiosemicarbazide (Figure 14(c))

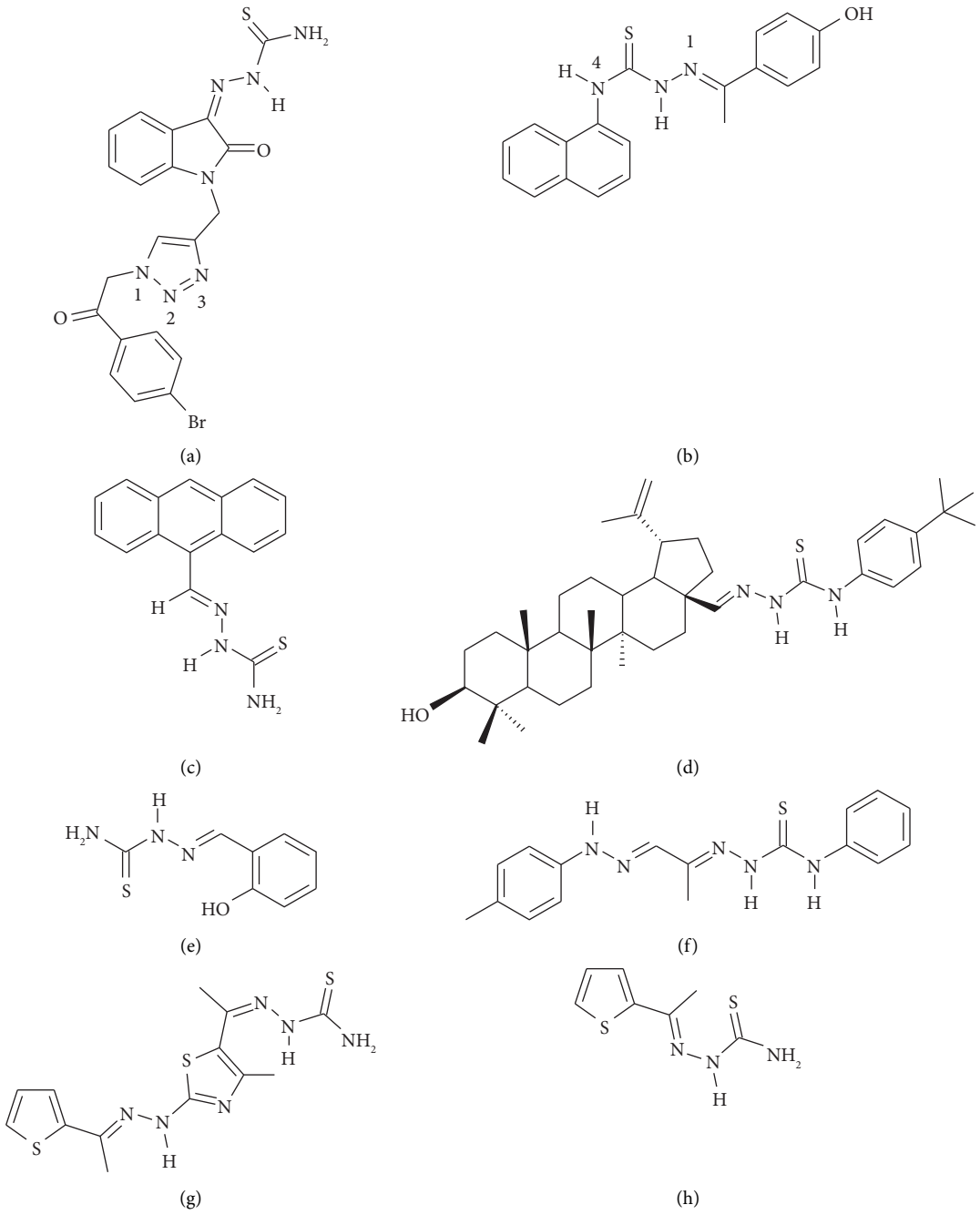

Figure 15: Structures of the comparative thiosemicarbazone derivatives II (a–h).

(IC_{50} = 53.4–64.5 and 46.5–71.3 μM, respectively) [53]. Besides, **5** was more cytotoxic than 3-methoxy-4-[2-(piperidine-1-yl)ethoxy)benzaldehyde thiosemicarbazone (Figure 14(d)) and 3-methoxy-4-[2-(morpholine-1-yl) ethoxy)benzaldehyde thiosemicarbazone (Figure 14(e)) with IC_{50} values > 100 uM against M-14 cells [54]. These evidences demonstrate that the *nitro* group attached to the furan ring at C-5 position in **5** favored the increase of the cytotoxicity in this studied cell line.

Compound **9** was found to be 3.8 and 9.8 times more active than 4-bromobenzomethyl-1,2,3-triazol-oxindol thiosemicarbazone (Figure 15(a)) (IC_{50} = 29.23 μM) and 4-(naphthalen-1-yl)-1-[1–(4-hydroxyphenyl)ethylidene) thiosemicarbazide (Figure 15(b)) (IC_{50} = 50.0–75.0 μM) assayed against LNCaP cells [55, 56]. In addition, **9** (IC_{50} = 34.84 μM) showed similar cytotoxic activity in comparison to anthracene-9-carbaldehyde thiosemicarbazone (Figure 15(c)) (IC_{50} = 33.71 μM) [57], Lup-20(29)-ene-3β-ol-28-N-(4-tert-butylphenyl) thiosemicarbazide (Figure 15(d)) (IC_{50} = 46.36 μM) [58] and salicylaldehyde thiosemicarbazone (Figure 15(e)) (IC_{50} = 45.20 μM) [59] and was more cytotoxic than (E)-N-phenyl-2-((E)-1-(2-(p-tolyl) hydrazono) propan-2- ylidene) hydrazine-1-carbothioamide (Figure 15(f)) (IC_{50} = 107.0 μg/mL) [35] and 2-(1-(4-

Table 7: Biological activity of the thiosemicarbazone derivatives **1**–**10** against Gram-positive bacteria and fungi strains determinated on the basis of MIC values, and scavenging DPPH radical activities determined on the basis of IC_{50} values.

Compounds	MIC[a] (μg/mL)							IC_{50}[b] (μg/mL)
	Gram-positive bacteria				Fungi			
	S. aureus ATCC43300	*S. aureus* ATCC29213	*S. aureus* ATCC25923	*S. aureus* ATCC700699	*C. albicans* ATCC90028	*C. albicans* ATCC10231	*C. albicans* ATCC750	DPPH activity
1	NA	NA	NA	NA	150	150	200	40.9 ± 0.2
2	NA	NA	NA	NA	150	150	200	NA
3	NA	NA	NA	NA	NA	NA	NA	NA
4	NA	NA	NA	NA	50	50	150	96.3 ± 5.0
5	10	10	25	1	NA	NA	NA	NA
6	NA	NA	NA	NA	NA	NA	NA	NA
7	NA	NA	NA	NA	NA	NA	NA	NA
8	NA	NA	NA	NA	NA	NA	NA	NA
9	NA	NA	NA	NA	NA	NA	NA	NA
10	NA	NA	NA	NA	NA	NA	NA	NA
Nitrofurantoin	2	25	25	1	—	—	—	—
Gentamicin	100	10	10	>100	—	—	—	—
Amphotericin B	—	—	—	—	5	5	100	
Nystatin	—	—	—	—	3	1	3	
Ascorbic acid	—	—	—	—	—	—	—	22.0 ± 0.1

[a]MIC: minimum inhibitory concentration; [b]IC_{50}: concentration of the compound (μg/mL) that causes a 50% DPPH scavenging after 48 h of compound exposure. The IC_{50} values are averages of three independent assays; NA: no activity; symbol (–): not tested.

methyl- 2-(2-(1-(thiophen-2-yl) ethylidene) hydrazinyl) thiazol-5-yl) ethylidene) hydrazinecarbothio-amide ($IC_{50} = 76.40\,\mu M$) (Figure 15(g)) [20] against breast adenocarcinoma cell line (MCF-7). Nevertheless, **8** ($IC_{50} = 53.96\,\mu M$) and **9** ($IC_{50} = 103.36\,\mu M$) tested against the duodenum adenocarcinoma HuTu80 cells were less cytotoxic than 2-acetylthiophene thiosemicarbazone (Figure 15(h)) ($IC_{50} = >10.0\,\mu M$) assayed *in vitro* on this same cell line [21].

3.4.2. Antibacterial Activity. All the synthesized thiosemicarbazones **1–10** and the standard drugs: Nitrofurantoin and Gentamicin were assayed for their antibacterial activity *in vitro* against four Grampositive bacterial strains: Methicillin and oxacillin-resistant *Staphylococcus aureus* ATCC 43300 and Methicillin -resistant *Staphylococcus aureus* (ATCC 29213, ATCC 25923, and ATCC 700699). The results of the *in vitro* antibacterial activities for the thiosemicarbazone derivatives **1–10** and the reference drugs are informed in Table 7.

All the prepared thiosemicarbazone derivatives were found to be inactive (MIC values > 200 μg/mL) in comparison to the Nitrofurantoin and Gentamicin standard drugs (Table 7), with the exception of compound **5** ($X = NO_2$) which exhibited better inhibitory activity against the *Staphylococcus aureus* ATCC43300, *Staphylococcus aureus* ATCC 29213 and *Staphylococcus aureus* ATCC 700699 strains (MIC = 10, 10 and 1 μg/mL, respectively). Furthermore, **5** was more effective than the indole-3- carbaldehyde-semicarbazone (MIC = 100—>200 μg/mL) [3], N′-4-methyl-N′-1-methylketone thiosemicarbazone (MIC = 39.68 —>50 μg/mL) [23], N′-4-phenyl-N′-2-acetylpyrazine thiosemicarbazone (MIC = 500 μg/mL) [24], N(4)-phenyl-N(1)-benzaldehyde thiosemicarbazone derivatives (MIC = 15.63–125 μg/mL) [60, 61] and 3-acetyl-2,5-dimethylthiophene thiosemicarbazone (MIC = 512 μg/mL) [25] derivatives, assayed against the *Staphylococcus aureus* strain. These evidences demonstrate that the NO_2 group attached at the furan ring of **5** favored the inhibition of bacterial growth.

3.4.3. Antifungal Activity. The *in vitro* antifungal activities of **1–10** were studied along with those of the standard Amphotericin and Nystatin. The microorganisms used in this study included 3 yeasts from *Candida* species, namely, *Candida albicans* ATCC 90028, *Candida albicans* ATCC 10231, and *Candida tropicalis* ATCC 750. The results of the *in vitro* antifungal activities for **1–10**, and the reference drugs, are listed in Table 7.

Among all the tested thiosemicarbazone derivatives, **4** ($X = 5\text{-}CF_3$) exhibited an acceptable antifungal activity (MIC = 50 μg/mL) against the *Candida albicans* (ATCC 90028 and ATCC 10231) strains. This evidence indicates that the CF_3 substituent at the C-5 positon of the furan ring could be producing an increase of the lipophilicity and enhanced the penetration of **4** into the lipid membrane and thus inhibits fungal growth [62]. However, **4** was less effective than the standard drugs Amphotericin B and Nystatin (MIC = 5 and 1–3 μg/mL, respectively). Compound **4** showed similar antifungal activity than the 2,3-dioxoindoline thiosemicarbazone derivatives (MIC = 30–60 μg/mL) tested against *Candida albicans* PTCC 5027 [63] and was more active than 1,3-bis-(2-carbaldehyde phenoxy) propan-2-ol ((MIC = 250 μg/mL) assayed against azole-sensitive *Candida albicans* ATCC 18804 [64]. Nevertheless, 2-((5-nitrothiophen-2-yl)methylene)-N-(pyridin-3-yl) hydrazine carbothioamide assayed against the *Candida albicans* ATCC 14053 strain was more effective (MIC = 4 μg/mL) [26] than **4**.

3.4.4. Antioxidant Activity. As shown in Table 7, **1** exhibited acceptable antioxidant activity ($IC_{50} = 40.9\,\mu g/mL$) as compared with the other tested thiosemicarbazone derivatives ($IC_{50} = 96.3–>100\,\mu g/mL$). However, **1** was less active in relation to the standard ascorbic acid ($IC_{50} = 22.0\,\mu g/mL$). In comparison to the antioxidant activity of 2-((5-nitrothiophen-2-yl) methylene)-N-(pyridin-3-yl) hydrazine carbothioamide using the DPPH method [26], **1** and **4** were 5.6 and 2.4 times more active. Based on the mentioned results, it is evident that the presence of the furan ring-bound thiosemicarbazone is important to increase the antioxidant activity. Compound **1** showed similar scavenging DPPH radical activity with respect to 1-[(E)-[(4-hydroxy-3-methoxyphenyl)methylidene]amino]-1methylthiourea and 1-methyl-1-[(E)-{[3-(trifluoromethyl) phenyl]methylidene}amino]thiourea [65]. On the other hand, **1** was less effective when evaluated as DPPH radical scavenger, in relation to 2-hydroxy-4-(N,N-diethylamino) benzaldehyde-4-(20-isocamphanyl) thiosemicarbazone containing the $N(CH_2CH_3)_2$ group (an electron-donating substituent) attached on the phenyl ring ($CE_{50} = 16.78\,\mu M$ or $6.76\,\mu g/mL$) [66].

4. Conclusion

In this work, ten furan-2-carbaldehyde thiosemicarbazone derivatives with different substituents were synthesized and characterized by mass spectrometry and FT-IR and NMR spectroscopic techniques. According to single crystal structure analyses, the crystal structures of **2**, **6,** and **7** exhibit *E* conformation around the N1-C6, N1-C11, and N1-C11 bonds, while the crystal structure of **8** shows *Z* conformation around the N1-C12 bond, involving an intramolecular N2-H. . .O2 hydrogen bond.

The antibacterial and antifungal data revealed that **5** exhibited good activity against the *Staphylococcus aureus* ATCC700699 compared to the Nitrofurantoin and Gentamicin reference drugs. On the other hand, **1** exhibited moderate effect of scavenging of DPPH radical with respect to the ascorbic acid reference compound. The new synthesized thiosemicarbazone derivatives were tested as candidate cytotoxic agents against different human tumor cells. Compound **5** showed moderate cytotoxic activity towards all tested cell lines, but it was particularly active at low micromolar concentrations against H460, HuTu80, MCF-7, and HT-29 cells, whereas compound **9** exhibited high cytotoxicity in comparison to the 5-fluorouracyl anticancer drug against the LNCaP cells and was more innocuous against 3T3 normal cells.

Our above mentioned results demonstrate that **5** is a promising candidate as antibacterial agent, while **5** and **9** can be considered as novel cytotoxic agents. These valuable findings should have a significant impact on the antibacterial and antitumor drugs development field.

Data Availability

CCDC 2235827 (3-Methyl-furan-2-carbaldehyde thiosemicarbazone, **2**), 2235828 (5-Phenyl-furan-2-carbaldehyde thiosemicarbazone, **6**), 2235829 (5-(2-Fluorophenyl)-furan-2-carbaldehyde thiosemicarbazone, **7**), and 2235830 (5-(4-Methoxyphenyl)-furan-2-carbaldehyde thiosemicarbazone, **8**) contain the supplementary crystallographic data. Copies of this information can be obtained free of charge from https://www.ccdc.cam.ac.uk/conts/retrieving.htlm.

Conflicts of Interest

The authors declare that there are no conflicts of interest with respect to the publication of this article.

Acknowledgments

WH and FC wish to acknowledge financial support from the Universidad de Lima Scientific Research Institute.

Supplementary Materials

Figure S1: ESI mass of **1**. Figure S2: FT-IR of **1**. Figure S3: ^{1}H NMR of **1**. Figure S4: ^{13}C NMR of **1**. Figure S5: ESI mass of **2**. Figure S6: FT-IR of **2**. Figure S7: ^{1}H NMR of **2**. Figure S8: ^{13}C NMR of **2**. Figure S9: Edited-2D ^{1}H-^{1}H NOESY of **2**. Figure S10: ESI mass of **3**. Figure S11: FT-IR of **3**. Figure S12: ^{1}H NMR of **3**. Figure S13: ^{13}C NMR of **3**. Figure S14: ESI mass of **4**. Figure S15: FT-IR of **4**. Figure S16: ^{1}H NMR of **4**. Figure S17: ^{13}C NMR of **4**. Figure S18: Edited-2D ^{1}H-^{1}H-NOESY of **4**. Figure S19: ESI mass of **5**. Figure S20: FT-IR of **5**. Figure 21: ^{1}H NMR of **5**. Figure 22: ^{13}C NMR of **5**. Figure 23: ESI mass of **6**. Figure 24: FT-IR of compound **6**. Figure 25: ^{1}H NMR of **6**. Figure 26: ^{13}C NMR of **6**. Figure 27: ESI mass of **7**. Figure 28: FT-IR of **7**. Figure 29: Edited-2D ^{1}H-^{13}C HSQC of **7**. Figure 30: ESI mass of **8**. Figure 31: FT-IR of **8**. Figure 32: ^{1}H NMR of **8**. Figure 33: ^{13}C NMR of **8**. Figure 34: Edited-2D ^{1}H-^{13}C HSQC of **8**. Figure 35: ESI mass of compound **9**. Figure 36: FT-IR of **9**. Figure 37: ^{1}H NMR of **9**. Figure 38: ^{13}C NMR of **9**. Figure 39: ESI mass of **10**. Figure 40: FT-IR of **10**. Figure 41: ^{1}H NMR of **10**. Figure 42: ^{13}C NMR of **10**. Table S1: Deviation from planarity: Data for least square planes calculated for compounds **2**, **6**, **7** and **8**. (*Supplementary Materials*)

References

[1] E. B. Noruzi, B. Shaabani, S. Geremia, N. Hickey, P. Nitti, and H. S. Kafil, "Synthesis, crystal structure, and biological activity of a multidentate calix[4]arene ligand doubly functionalized by 2-hydroxybenzeledene- thiosemicarbazone," *Molecules*, vol. 25, no. 2, pp. 1–19, 2020.

[2] K. Jayanthi, R. P. Meena, K. Chithra et al., "Synthesis and microbial evaluation of copper(II) complexes of schiff base ligand derived from 3-methoxysalicylaldehyde with semicarbazide and thiosemicarbazide," *Journal of Pharmaceutical, Chemical and Biological Sciences*, vol. 5, no. 3, pp. 205–215, 2017.

[3] F. Carrasco, W. Hernández, O. Chupayo et al., "Indole-3-carbaldehyde semicarbazone derivatives: synthesis, characterization, and antibacterial activities," *Journal of Chemistry*, vol. 2020, Article ID 7157281, 9 pages, 2020.

[4] F. Bisceglie, F. Degola, D. Rogolino et al., "Sisters in structure but different in character, some benzaldehyde and cinnamaldehyde derivatives differentially tune *Aspergillus flavus* secondary metabolism," *Scientific Reports*, vol. 10, no. 1, pp. 17686–17714, 2020.

[5] J. D. N. A. Camargo, K. E. Pianoski, M. G. dos Santos et al., "Antiparasitic behavior of trifluoromethylated pyrazole 2-amino-1,3,4-thiadiazole hybrids and their analogues: synthesis and structure-activity relationship," *Frontiers in Pharmacology*, vol. 11, Article ID 591570, 2020.

[6] K. Gobis, M. Szczesio, A. Olczak et al., "N'-Substituted 4-phenylpicolinohydrazonamides with thiosemicarbazone moiety as new potential antitubercular agents: synthesis, structure and evaluation of antimicrobial activity," *Materials*, vol. 15, no. 16, p. 5513, 2022.

[7] F. Carrasco, W. Hernández, O. Chupayo et al., "Phenyl-isoxazole-3/5-Carbaldehyde isonicotinylhydrazone derivatives: synthesis, characterization, and antitubercular activity," *Journal of Chemistry*, vol. 2021, Article ID 6014093, 14 pages, 2021.

[8] S. Y. Abbas, W. M. Tohamy, W. M. Basyouni et al., "Design, synthesis and antiviral evaluation of new *N*-(4)-(benzo[d][1,3]-dioxol-5-yl)thiosemicarbazone derivatives," *Egyptian Journal of Chemistry*, vol. 10, 3800 pages, 2021.

[9] V. Francesconi, E. Cichero, S. Schenone, L. Naesens, and M. Tonelli, "Synthesis and biological evaluation of novel (thio) semicarbazone-Based benzimidazoles as antiviral agents against human respiratory viruses," *Molecules*, vol. 25, no. 7, p. 1487, 2020.

[10] L. Sens, A. S. Oliveira, A. Mascarello, I. M. C. Brighente, R. A. Yunes, and R. J. Nunes, "Synthesis, antioxidant activity, acetylcholinesterase inhibition and quantum studies of thiosemicarbazones," *Journal of the Brazilian Chemical Society*, vol. 29, no. 2, pp. 343–352, 2018.

[11] S. Eğlence-Bakir, "Synthesis and antioxidant activities of new nickel(II) complexes derived from 4-benzyloxysalicylidene-S-methyl/propyl thiosemicarbazones," *Turkish Journal of Chemistry*, vol. 45, no. 3, pp. 835–844, 2021.

[12] C. G. Oliveira, I. Romero-Canelón, J. P. C. Coverdale et al., "Novel tetranuclear Pd(II) and Pt(II) anticancer complexes derived from pyrene thiosemicarbazones," *Dalton Transactions*, vol. 49, no. 28, pp. 9595–9604, 2020.

[13] J. Qi, T. Liu, W. Zhao, X. Zheng, and Y. Wang, "Synthesis, crystal structure and antiproliferative mechanisms of gallium(III) complexes with benzoylpyridine thiosemicarbazones," *Royal Society of Chemistry Advances*, vol. 10, pp. 18553–18559, 2020.

[14] M. Niso, J. Kopecka, F. S. Abatematteo, F. Berardi, C. Riganti, and C. Abate, "Multifunctional thiosemicarbazones targeting sigma receptors: *in vitro* and *in vivo* antitumor activities in pancreatic cancer models," *Cellular Oncology*, vol. 44, no. 6, pp. 1307–1323, 2021.

[15] I. Kostova and L. Saso, "Advances in research of schiff-base metal complexes as potent antioxidants," *Current Medicinal Chemistry*, vol. 20, no. 36, pp. 4609–4632, 2013.

[16] T. P. Stanojkovic, D. Kovala-Demertzi, A. Primikyri et al., "Zinc(II) complexes of 2-acetyl pyridine 1-(4-fluorophenyl)-piperazinyl thiosemicarbazone: synthesis, spectroscopic study and crystal structures – potential anticancer drugs," *Journal of Inorganic Biochemistry*, vol. 104, no. 4, pp. 467–476, 2010.

[17] M. Pitucha, A. Korga-Plewko, A. Czylkowska et al., "Influence of complexation of thiosemicarbazone derivatives with Cu (II) ions on their antitumor activity against melanoma cells," *International Journal of Molecular Sciences*, vol. 22, no. 6, pp. 3104–3111, 2021.

[18] O. Dömötör, M. A. Kiss, G. T. Gál et al., "Solution equilibrium, structural and cytotoxicity studies on Ru(η6-*p*-cymene) and copper complexes of pyrazolyl thiosemicarbazones," *Journal of Inorganic Biochemistry*, vol. 202, Article ID 110883, 2020.

[19] F. Vandresen, S. A. D. Almeida-Batista, M. E. B. Caldeira et al., "Antitumor and antileishmanial activities of limonene-thiosemicarbazones bearing heterocycles nucleous," *Research, Society and Development*, vol. 11, no. 5, 2022.

[20] S. M. Gomha, H. A. Abdelhady, D. Z. H. Hassain et al., "Thiazole-Based thiosemicarbazones: synthesis, cytotoxicity evaluation and molecular docking study," *Drug Design, Development and Therapy*, vol. 15, pp. 659–677, 2021.

[21] A. A. Ali, H. Nimir, C. Aktas et al., "Organoplatinum(II) complexes with 2-acetylthiophene thiosemicarbazone: synthesis, characterization, crystal structures, and in vitro antitumor activity," *Organometallics*, vol. 31, no. 6, pp. 2256–2262, 2012.

[22] W. Hernández, F. Carrasco, A. Vaisberg et al., "Synthesis, spectroscopic characterization, structural studies, and in vitro antitumor activities of pyridine-3-carbaldehyde thiosemicarbazone derivatives," *Journal of Chemistry*, vol. 2020, Article ID 2960165, 12 pages, 2020.

[23] I. D'Agostino, G. E. Mathew, P. Angelini et al., "Biological investigation of *N*-methyl thiosemicarbazones as antimicrobial agents and bacterial carbonic anhydrases inhibitors," *Journal of Enzyme Inhibition and Medicinal Chemistry*, vol. 37, no. 1, pp. 986–993, 2022.

[24] D. Polo-Cerón, "Cu(II) and Ni(II) complexes with new tridentate NNS thiosemicarbazones: synthesis, characterisation, DNA interaction, and antibacterial activity," *Bioinorganic Chemistry and Applications*, vol. 2019, Article ID 3520837, 14 pages, 2019.

[25] S. A. Khan, A. M. Asiri, K. Al-Amry, and M. A. Malik, "Synthesis, characterization, electrochemical studies, and *in vitro* antibacterial activity of novel thiosemicarbazone and its Cu(II), Ni(II), and Co(II) complexes," *The Scientific World Journal*, vol. 2014, Article ID 592375, 9 pages, 2014.

[26] L. N. Araújo Neto, M. C. A. Lima, J. F. Oliveira et al., "Thiophene-thiosemicarbazone derivative (L10) exerts antifungal activity mediated by oxidative stress and apoptosis in *C. albicans*," *Chemico-Biological Interactions*, vol. 320, 2020.

[27] Stoe & Cie GmbH, *X-area Version 1.90*, Stoe & Cie GmbH, Darmstadt, Germany, 2020.

[28] G. M. Sheldrick, "SHELXT-Integrated space-group and crystal-structure determination," *Acta Crystallographica A71*, vol. 71, pp. 3–8, 2015.

[29] G. M. Sheldrick, "A short history of SHELX," *Acta Crystallographica Section A Foundations of Crystallography*, vol. 64, no. 1, pp. 112–122, 2008.

[30] K. Brandenburg, *Diamond Version 4.3.0*, Crystal Impact GbR, Bonn, Germany, 2016.

[31] P. Skehan, R. Storeng, D. Scudiero et al., "New colorimetric cytotoxicity assay for anticancer-drug screening," *JNCI Journal of the National Cancer Institute*, vol. 82, no. 13, pp. 1107–1112, 1990.

[32] C. Tamariz-Angeles, P. Olivera-Gonzales, and M. Santillán-Torres, "Antimicrobial, antioxidant and phytochemical assessment of wild medicinal plants from Cordillera Blanca (Ancash, Peru)," *Boletin Latinoamericano y del Caribe de Plantas Medicinales y Aromaticas*, vol. 17, no. 3, pp. 270–285, 2018.

[33] S. Sardari, S. Feizi, A. H. Rezayan et al., "Synthesis and biological evaluation of thiosemicarbazide derivatives endowed with high activity toward *Mycobacterium bovis*," *Iranian Journal of Pharmaceutical Research: International Journal of Psychological Research*, vol. 16, no. 3, pp. 1128–1140, 2017.

[34] S. Guler, H. A. Kayali, E. O. Sadan, B. Sen, and E. Subasi, "Half-sandwich arene ruthenium(II) thiosemicarbazone complexes: evaluation of anticancer effect on primary and metastatic ovarian cancer cell lines," *Frontiers in Pharmacology*, vol. 13, Article ID 882756, 2022.

[35] A. A. El-Sisi, M. Ali, S. F. Ramdan, O. AlTaweel, A. I. A. Abd El-Mageed, and A. A. El-Sherif, "Synthesis, characterization, X-ray single-crystal structure, potentiometric measurements, molecular modeling, and bioactivity screening of some thiosemicarbazones," *Journal of Chemistry*, vol. 2022, Article ID 1241470, 2115 pages, 2022.

[36] F. El-Saied, B. El-Aarag, T. Salem, G. Said, S. A. M. Khalifa, and H. R. El-Seedi, "Synthesis, characterization, and in vivo anti-cancer activity of new metal complexes derived fromIsatin-N(4)antipyrinethiosemicarbazone ligand against ehrlich ascites carcinoma cells," *Molecules*, vol. 24, no. 18, p. 3313, 2019.

[37] E. Pahontu, V. Fala, A. Gulea, D. Poirier, V. Tapcov, and T. Rosu, "Synthesis and characterization of some new Cu(II), Ni(II) and Zn(II) complexes with salicylidene thiosemicarbazones: antibacterial, antifungal and *in vitro* antileukemia activity," *Molecules*, vol. 18, no. 8, pp. 8812–8836, 2013.

[38] A. I. Matesanz, C. Hernández, and P. Souza, "New bioactive 2,6-diacetylpyridine bis(p-chlorophenylthiosemicarbazone) ligand and its Pd(II) and Pt(II) complexes: synthesis, characterization, cytotoxic activity and DNA binding ability," *Journal of Inorganic Biochemistry*, vol. 138, pp. 16–23, 2014.

[39] K. S. O. Ferraz, J. G. Da Silva, F. M. Costa et al., "N(4)-Tolyl-2-acetylpyridine thiosemicarbazones and their platinum(II,IV) and gold(III) complexes: cytotoxicity against human glioma cells and studies on the mode of action," *Biometals*, vol. 26, no. 5, pp. 677–691, 2013.

[40] P. Vijayan, P. Viswanathamurthi, V. Silambarasan et al., "Dissymmetric thiosemicarbazone ligands containing substituted aldehyde arm and their ruthenium(II) carbonyl complexes with PPh_3/$AsPh_3$ as ancillary ligands: synthesis, structural characterization, DNA/BSA interaction and *in vitro* anticancer activity," *Journal of Organometallic Chemistry*, vol. 768, pp. 163–177, 2014.

[41] B. Sever, H. S. S. Görgülü, Z. Cantürk, and M. D. Altintop, "Pyrazole incorporated new thiosemicarbazones: design, synthesis and investigation of DPP-4 inhibitory effects," *Molecules*, vol. 25, no. 21, pp. 1–19, 2020.

[42] M. A. Hussein, T. S. Guan, R. A. Haque, M. B. Khadeer Ahamed, and A. M. Abdul Majid, "Mononuclear dioxomolybdenum(VI) thiosemicarbazonato complexes: synthesis,

characterization, structural illustration, *in vitro* DNA binding, cleavage, and antitumor properties," *Spectrochimica Acta Part A: Molecular and Biomolecular Spectroscopy*, vol. 136, pp. 1335–1348, 2015.

[43] J. Haribabu, S. Srividya, D. Mahendiran et al., "Synthesis of palladium(II) complexes via michael addition: antiproliferative effects through ROS-mediated mitochondrial apoptosis and docking with SARS-CoV-2," *Inorganic Chemistry*, vol. 59, no. 23, pp. 17109–17122, 2020.

[44] G. L. Parrilha, K. S. O. Ferraz, J. A. Lessa et al., "Metal complexes with 2-acetylpyridine-N(4)-ortho-chlorophenylthiosemicarbazone: cytotoxicity and effect on the enzymatic activity of thioredoxin reductase and glutathione reductase," *European Journal of Medicinal Chemistry*, vol. 84, pp. 537–544, 2014.

[45] W. Hernández, J. Paz, F. Carrasco et al., "Synthesis and characterization of new palladium(II) complexes with ligands derived from furan-2-carbaldehyde and benzaldehyde thiosemicarbazone and their *in vitro* cytotoxic activities against various human tumor cell lines," *Zeitschrift für Naturforschung B*, vol. 65, no. 10, pp. 1271–1278, 2010.

[46] A. A. Ibrahim, H. Khaledi, P. Hassandarvish, H. Mohd Ali, and H. Karimian, "Indole-7-carbaldehyde thiosemicarbazone as a flexidentate ligand toward Zn^{II}, Cad^{II}, Pd^{II} and Pt^{II} ions: cytotoxic and apoptosis-inducing properties of the Pt^{II} complex," *Dalton Transactions*, vol. 43, no. 10, pp. 3850–3860, 2014.

[47] E. Pahontu, F. Julea, T. Rosu et al., "Antibacterial, antifungal and in vitro antileukaemia activity of metal complexes with thiosemicarbazones," *Journal of Cellular and Molecular Medicine*, vol. 19, no. 4, pp. 865–878, 2015.

[48] V. Graur, Y. Chumakov, O. Garbuz, C. Hureau, V. Tsapkov, and A. Gulea, "Synthesis, structure, and biologic activity ofSome copper, nickel, cobalt, and zinc complexes with 2-formylpyridine N4-allylthiosemicarbazone bioinorganic chemistry and applications," *Bioinorganic Chemistry and Applications*, vol. 2022, Article ID 2705332, 18 pages, 2022.

[49] A. I. Matesanz, I. Leitao, and P. Souza, "Palladium(II) and platinum(II) bis(thiosemicarbazone) complexes of the 2,6-diacetylpyridine series with high cytotoxic activity in cisplatin resistant A2780cisR tumor cells and reduced toxicity," *Journal of Inorganic Biochemistry*, vol. 125, pp. 26–31, 2013.

[50] W. Hernández, A. J. Vaisberg, M. Tobar et al., "In vitro antiproliferative activity of palladium(II) thiosemicarbazone complexes and the corresponding functionalized chitosan coated magnetite nanoparticles," *New Journal of Chemistry*, vol. 40, no. 2, pp. 1853–1860, 2016.

[51] W. Hernández, J. Paz, A. Vaisberg, E. Spodine, R. Richter, and L. Beyer, "Synthesis and characterization of new palladium(II) thiosemicarbazone complexes and their cyotoxic activity against various human tumor cell lines," *Bioinorganic Chemistry and Applications*, vol. 2013, Article ID 524701, 12 pages, 2013.

[52] K. M. Roque Marques, M. R. do Desterro, S. M. de Arruda et al., "5-Nitro-Thiophene-Thiosemicarbazone derivatives present antitumor activity mediated by apoptosis and DNA intercalation," *Current Topics in Medicinal Chemistry*, vol. 19, no. 13, pp. 1075–1091, 2019.

[53] F. Vandresen, H. Falzirolli, S. A. Almeida Batista et al., "Novel R-(+)-limonene-based thiosemicarbazones and their antitumor activity against human tumor cell lines," *European Journal of Medicinal Chemistry*, vol. 79, pp. 110–116, 2014.

[54] D. E. S. Silva, A. B. Becceneri, J. V. Santiago et al., "Silver(I) complexes of 3-methoxy-4-hydroxybenzaldehyde thiosemicarbazones and triphenylphosphine: structural, cytotoxicity, and apoptotic studies," *Dalton Transactions*, vol. 49, no. 45, pp. 16474–16487, 2020.

[55] S. Nazari, F. Safari, M. B. Mamaghani, and A. Bazgir, "Synthesis and evaluation of in vitro cytotoxic effects of triazol/spiroindolinequinazolinedione, triazol/indolin-3-thiosemicarbazone and triazol/thiazol-indolin-2-one conjugates," *Daru Journal of Pharmaceutical Sciences*, vol. 28, no. 2, pp. 591–601, 2020.

[56] M. D. Altintop, B. Sever, A. Özdemir et al., "Synthesis and evaluation of naphthalene-based thiosemicarbazone derivatives as new anticancer agents against LNCaP prostate cancer cells," *Journal of Enzyme Inhibition and Medicinal Chemistry*, vol. 31, no. 3, pp. 410–416, 2016.

[57] J. Bai, R. H. Wang, Y. Qiao, A. Wang, and C. J. Fang, "Schiff base derived from thiosemicarbazone and anthracene showed high potential in overcoming multidrug resistance in vitro with low drug resistance index," *Drug Design, Development and Therapy*, vol. 11, pp. 2227–2237, 2017.

[58] J. Wang, J. Wu, Y. Han et al., "Design and synthesis of novel betulin derivatives containing thio-/semicarbazone moieties as apoptotic inducers through mitochindria-related pathways," *Molecules*, vol. 26, no. 21, p. 6356, 2021.

[59] T. V. Petrasheuskaya, M. A. Kiss, O. Dömötör et al., "Salicylaldehyde thiosemicarbazone copper complexes: impact of hybridization with estrone on cytotoxicity, solution stability and redox activity," *New Journal of Chemistry*, vol. 44, no. 28, pp. 12154–12168, 2020.

[60] J. D. Londoño-Mosquera, A. Aragón-Muriel, and D. Polo-Cerón, "Synthesis, antibacterial activity and DNA interactions of lanthanide(III) complexes of N(4)-substituted thiosemicarbazones," *Universitas Scientiarum*, vol. 23, no. 2, pp. 141–169, 2018.

[61] N. Trotsko, U. Kosikowska, A. Paneth, T. Plech, A. Malm, and M. Wujec, "Synthesis and antibacterial activity of new thiazolidine-2,4-dione-based chlorophenylthiosemicarbazone hybrids," *Molecules*, vol. 23, no. 5, pp. 1023–1117, 2018.

[62] C. Bonaccorso, T. Marzo, and D. La Mendola, "Biological applications of thiocarbohydrazones and their metal complexes: a perspective review," *Pharmaceuticals*, vol. 13, no. 1, p. 19, 2020.

[63] S. Mohebbi, M. Hassan, R. Ghaffari, S. Sardari, and Y. Farahani, "Discovery of novel isatin-based thiosemicarbazones: synthesis, antibacterial, antifungal, and antimycobacterial screening," *Research in Pharmaceutical Sciences*, vol. 15, no. 3, pp. 281–290, 2020.

[64] R. M. Kassab, S. M. Gomha, S. A. Al-Hussain et al., "Synthesis and in-silico simulation of some new bis-thiazole derivatives and their preliminary antimicrobial profile: investigation of hydrazonoyl chloride addition to hydroxy-functionalized bis-carbazones," *Arabian Journal of Chemistry*, vol. 14, no. 11, pp. 103396–103414, 2021.

[65] N. Sharma and D. P. Pathak, "Synthesis and characterization of novel benzaldehyde thiosemicarbazones and evaluation of their antibacterial, antifungal and antioxidant activity," *International Journal of Pharmaceutical Sciences and Research*, vol. 8, no. 2, pp. 667–678, 2017.

[66] L. Yang, H. Liu, D. Xia, and S. Wang, "Antioxidant properties of camphene-based thiosemicarbazones: experimental and theoretical evaluation," *Molecules*, vol. 25, no. 5, pp. 1–16, 2020.